4a Technology Day 2020

Material Characterization and Experimental Validation of UD CFRP Laminate Components using LS-DYNA®

M. Nishi, M. Iimori, K. Saito

T. Nishihara, C. Kawamura, S. Kanemoto

JSOL

NTT DATA Trusted Global Innovator
NTT DATA Group

JSOL ICT Service Coordinator

- Company name: JSOL Corporation
- Established: July,2006
- Capital: 5 billion yen
- Employees: 1,200
- Shareholder: NTT DATA Corporation
  The Japan Research Institute, Limited
- Offices: Tokyo Head Office
  Osaka Head Office
  Nagoya Branch Offices
- Business Field

Industrial Field Solution

Financial field Solution

Public Sector Solution

CAE Solution

IT Consulting

Outline

1. Background & Motivation
2. FE Modeling
3. Material Characterization
4. 1st Experimental Validation
5. Review and Improvement of FE Modeling
6. 2nd Experimental Validation
7. Summary & Future Work

Outline

1. **Background & Motivation**
2. FE Modeling
3. Material Characterization
4. 1st Experimental Validation
5. Review and Improvement of FE Modeling
6. 2nd Experimental Validation
7. Summary & Future Work

Background of the Study

Joint research project with Mazda and JSOL

Mazda is interested in CFRP as one of the break-through technologies that achieves a high level of downsizing, weight reduction and safety.

CFRP is light,

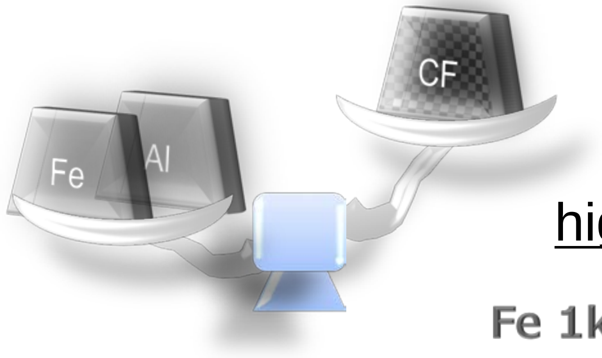

high specific strength

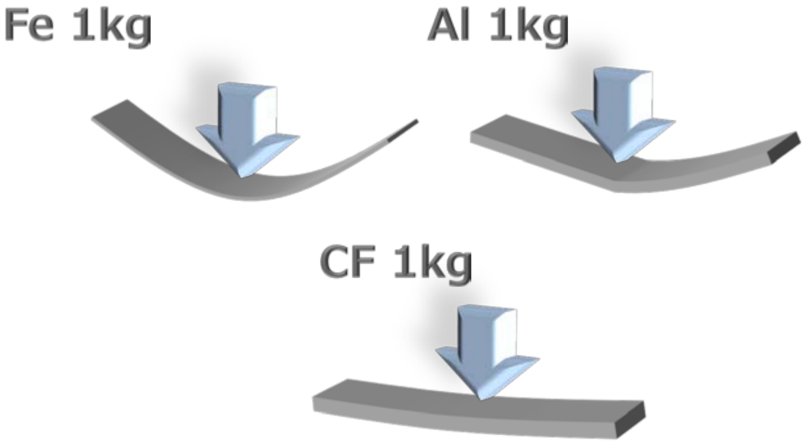

has energy absorption characteristics close to ideal

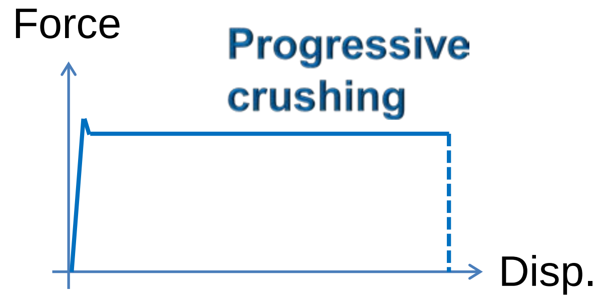

Crash Simulations for Passive Safety

Crash simulation is especially important in automotive design because of the strict regulations which specify passive safety requirements.

Full Frontal Impact

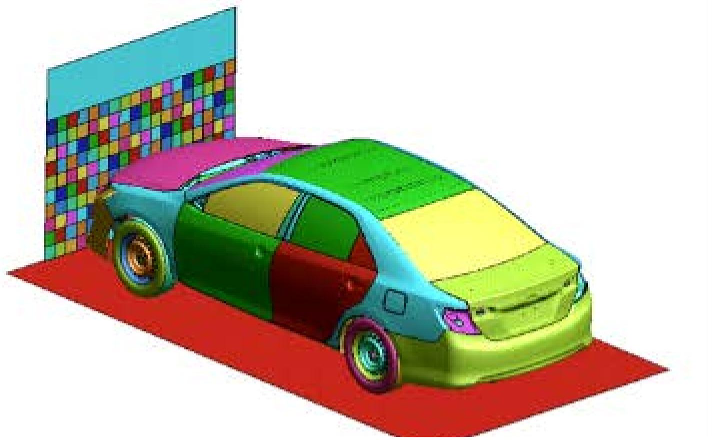

ODB Frontal Impact

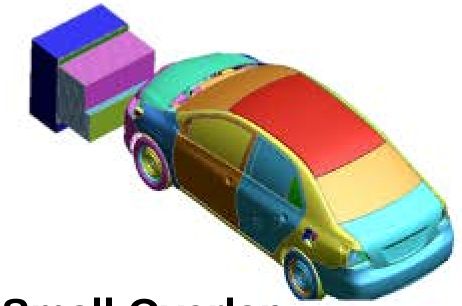

Side Barrier Impact

IIHS Small Overlap

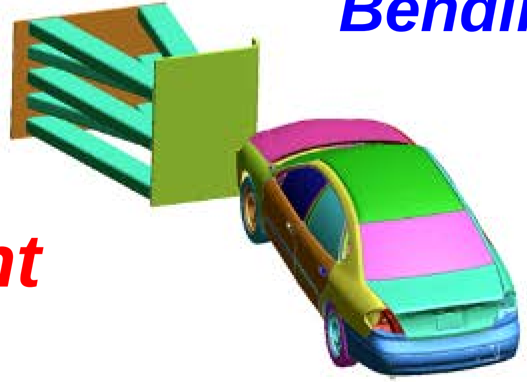

Bending dominant

Side Pole Impact

Compression dominant

The numerical predictions of bending fracture and axial crushing of a composite structure are both of great interest with CFRP composites being increasingly applied in car design.

Requirements and Motivation

Requirements for Numerical Simulation

Design Parameters

- tube geometry
- laminate configuration
- material

Crash Conditions

- Velocity
- Temperature

Failure Modes

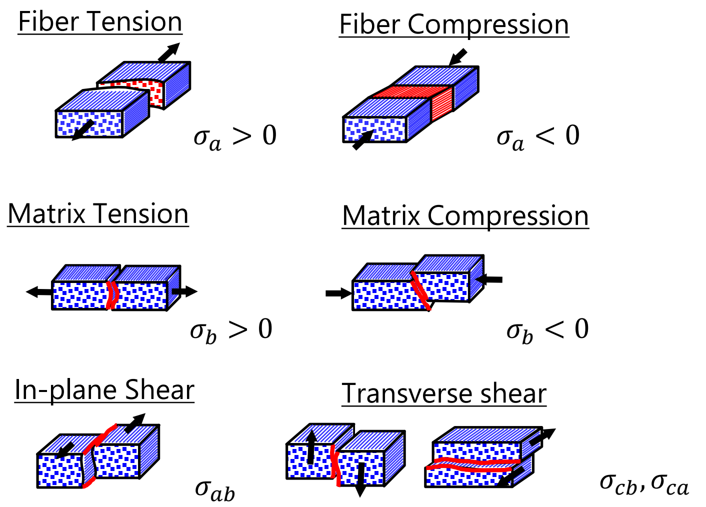

Crash Performance

- Reaction Force
- Energy Absorption

Motivations of this Study

- To validate the simulated **failure mode** by FE simulation when design parameters, including **laminate configuration**, are changed.

Outline

1. Background & Motivation
2. **FE Modeling**
3. Material Characterization
4. 1st Experimental Validation
5. Review and Improvement of FE Modeling
6. 2nd Experimental Validation
7. Summary & Future Work

Laminate Modeling

In terms of modeling that can be calculated by realistic computational costs, we selected the multi-layered shell model.

laminated composite

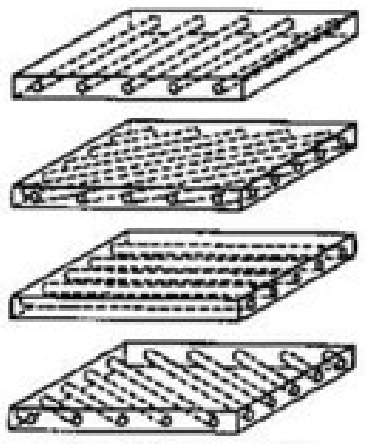

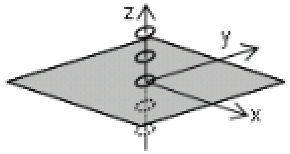

Single-layered shell elements (*PART_COMPOSITE)

+ numerically “cheap” (applicable to full vehicle model)
- can not represent “delamination”

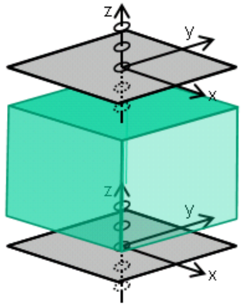

Multi-layered shell elements

+ can represent “delamination”
+ still acceptable computation cost

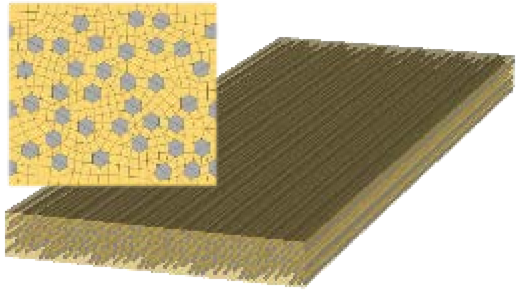

Micro/Meso-scale model

+ directly captures the complex failure mode
- huge computation cost is needed

Intra-lamina Modeling

Material model in each ply needs to treat the CFRP as an anisotropic homogeneous material.

Requirements for CFRP Material Model

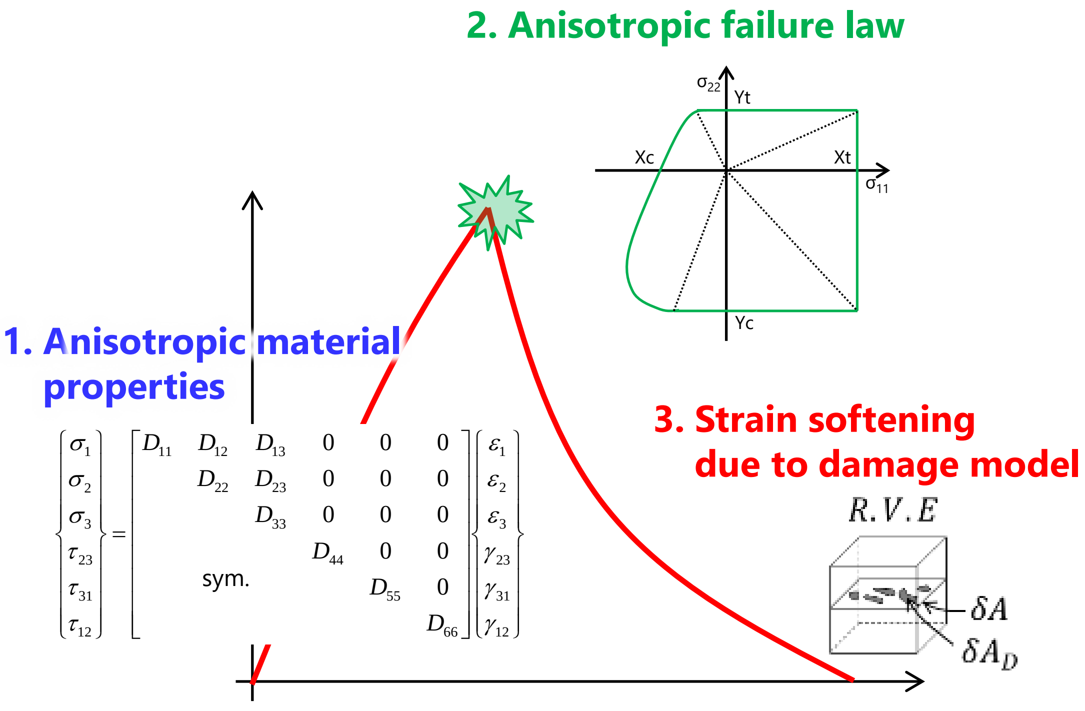

$$\begin{Bmatrix}\sigma_1\\ \sigma_2\\ \sigma_3\\ \tau_{23}\\ \tau_{31}\\ \tau_{12}\end{Bmatrix} = \begin{bmatrix} D_{11} & D_{12} & D_{13} & 0 & 0 & 0\\ & D_{22} & D_{23} & 0 & 0 & 0\\ & & D_{33} & 0 & 0 & 0\\ & & & D_{44} & 0 & 0\\ & \text{sym.} & & & D_{55} & 0\\ & & & & & D_{66}\end{bmatrix} \begin{Bmatrix}\varepsilon_1\\ \varepsilon_2\\ \varepsilon_3\\ \gamma_{23}\\ \gamma_{31}\\ \gamma_{12}\end{Bmatrix}$$

*MAT_054/058

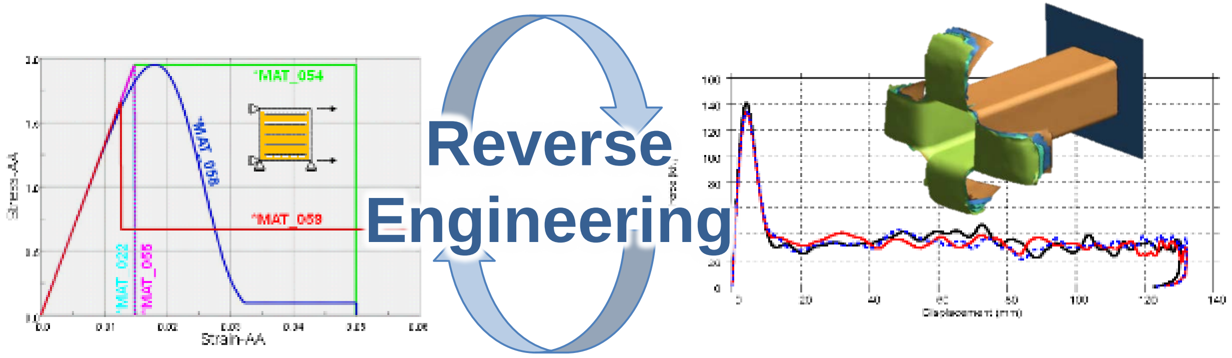

*MAT_261/262

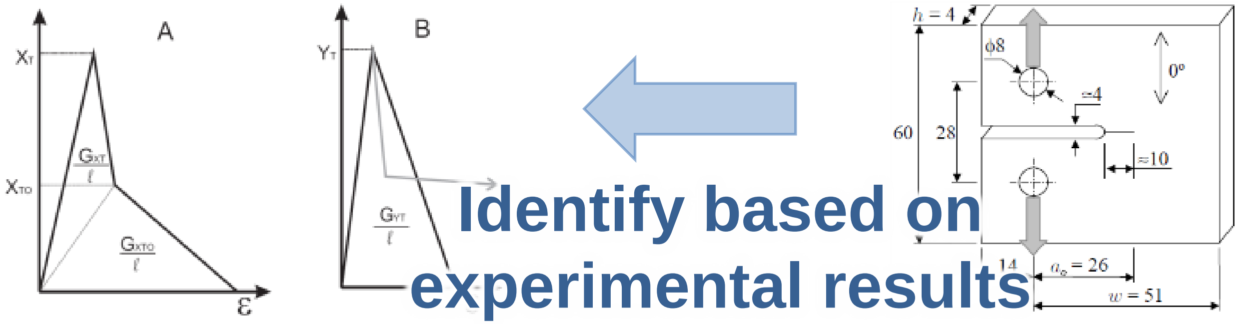

FE Modeling

We selected in the project.

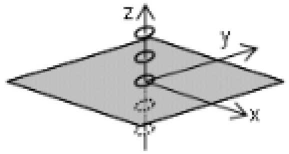

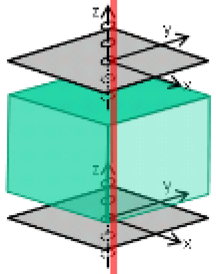

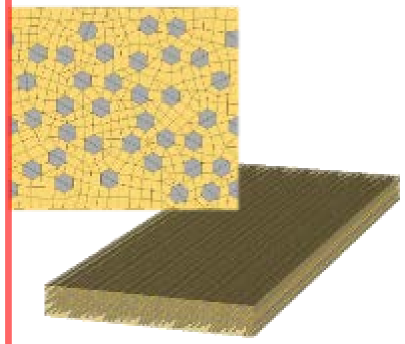

	Single-layered shell elements with *PART_COMPOSITE		Multi-layered shell elements with cohesive elements		Micro/Meso scale model
	*MAT_054/058	*MAT_261/262	*MAT_054/058	*MAT_261/262	
Lamination configuration	✓	✓	✓	✓	✓
Delamination			✓	✓	✓
Crack propagation		✓		✓	✓
Computation cost	Full vehicle level		Component level		RVE level

Outline

1. Background & Motivation
2. FE Modeling
3. **Material Characterization**
4. 1st Experimental Validation
5. Review and Improvement of FE Modeling
6. 2nd Experimental Validation
7. Summary & Future Work

Intra-laminar parameters

Toray 3252S-10 (T700/2592)

*MAT_LAMINATED_FRACTURE_DAIMLER_CAMANHO (262)

Card 1

		E_1	E_2		v_{21}	v_{31}	v_{32}

Card 2

G_{12}	G_{23}	G_{31}

Card 5

G_{XC}	G_{XT}	G_{YC}	G_{YT}	G_{SL}	G_{XCO}	G_{XTO}

Card 6

X_C	X_T	Y_C	Y_T	S_L	X_{CO}	X_{TO}

Card 7

	σ_y	E_{tan}

Tensile coupon test in 0, 45, 90 direction

Tensile coupon test in 0, 45, 90 direction

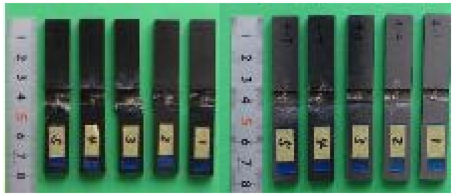

Compressive coupon test in 0, 90 direction

4-pint bending ENF test

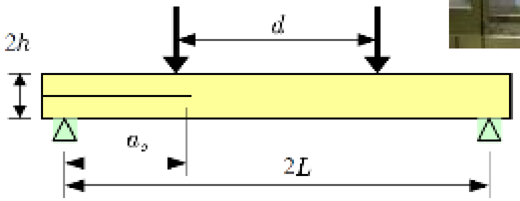

DCB test

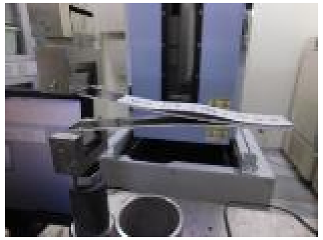

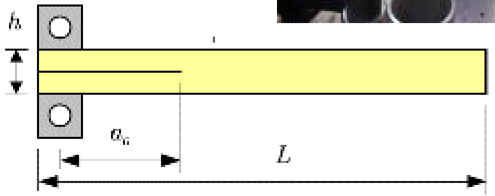

Intra-laminar parameters

Toray 3252S-10 (T700/2592)

*MAT_LAMINATED_FRACTURE_DAIMLER_CAMANHO (262)

Card 1

		E_1	E_2		v_{21}	v_{31}	v_{32}

Card 2

G_{12}	G_{23}	G_{31}

Card 5

G_{XC}	G_{XT}	G_{YC}	G_{YT}	G_{SL}	G_{XCO}	G_{XTO}

Card 6

X_C	X_T	Y_C	Y_T	S_L	X_{CO}	X_{TO}

	σ_y	E_{tan}

Double notched compressive test

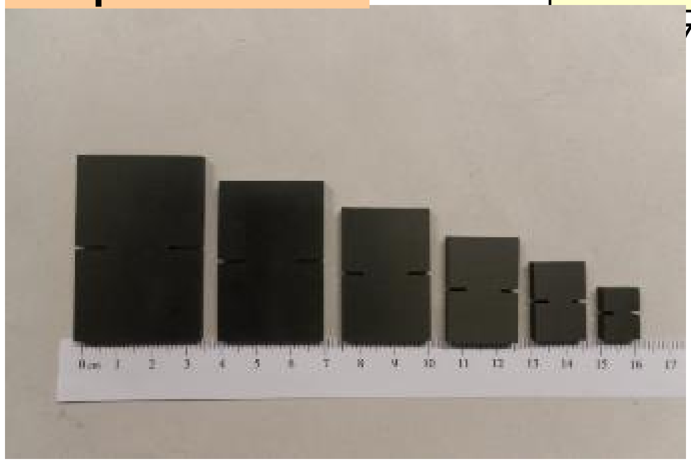

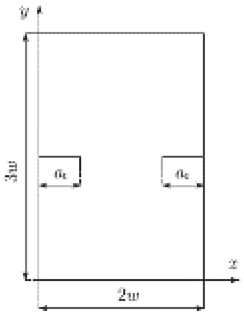

Double notched tensile test

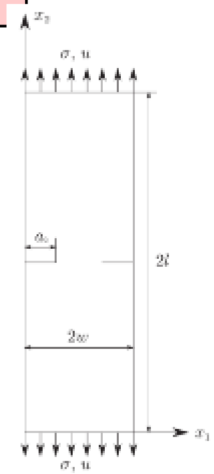

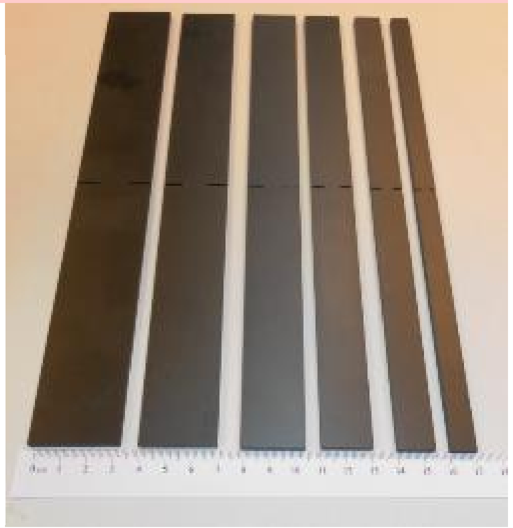

Intra-laminar parameters

Compressive damage parameters in fiber direction

Double notched compressive test

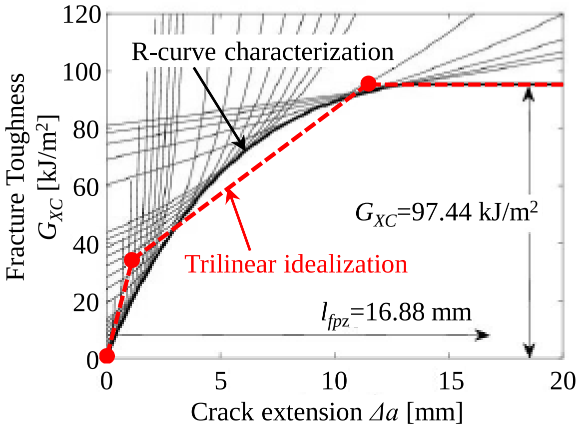

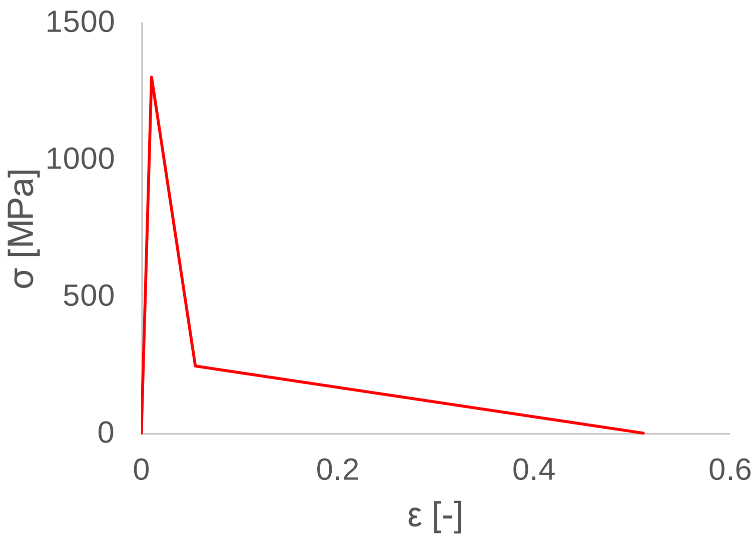

Characterization of R-curve using size effect of fracture (G. Catalanotti et. al., 2014)

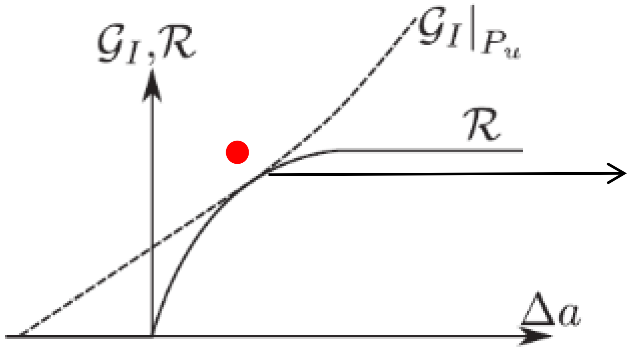

Identification of bi-linear damage properties (Carlos G. Dávila et. al., 2009)

$$G_M(\Delta a) = \begin{cases} \frac{3}{2}\frac{\Delta a}{l_c} G_c & if \ \frac{\Delta a}{l_c} \le \frac{3}{2}\frac{m}{n} \\ mG_c + (1-n)\frac{3}{2}\frac{\Delta a}{l_c} G_c & if \ \frac{3}{2}\frac{m}{n} < \frac{\Delta a}{l_c} < \frac{3}{2}\frac{1-m}{1-n} \\ G_c & if \ \frac{\Delta a}{l_c} \ge \frac{3}{2}\frac{1-m}{1-n} \end{cases}$$

Intra-laminar parameters

Tensile damage parameters in fiber direction

Double notched tensile test

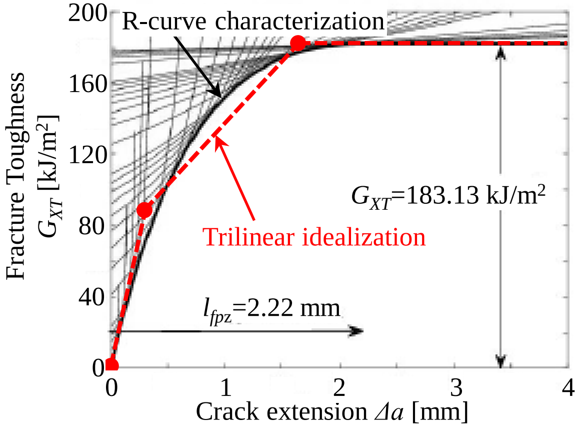

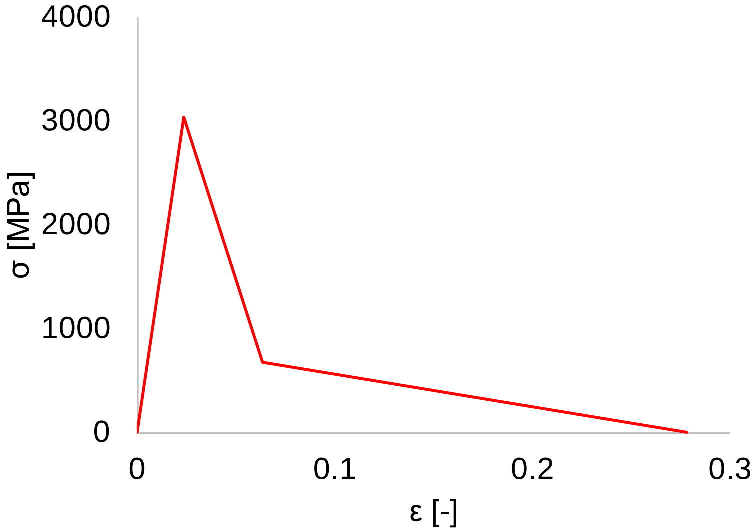

Characterization of R-curve using size effect of fracture (G. Catalanotti et. al., 2014)

Identification of bi-linear damage properties (Carlos G. Dávila et. al., 2009)

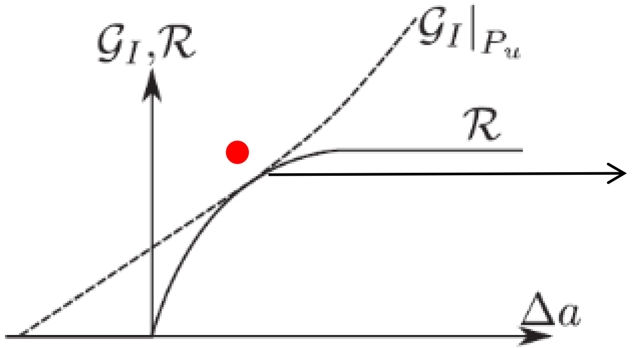

$$G_M(\Delta a) = \begin{cases} \frac{3}{2}\frac{\Delta a}{l_c} G_c & if \ \frac{\Delta a}{l_c} \le \frac{3}{2}\frac{m}{n} \\ mG_c + (1-n)\frac{3}{2}\frac{\Delta a}{l_c} G_c & if \ \frac{3}{2}\frac{m}{n} < \frac{\Delta a}{l_c} < \frac{3}{2}\frac{1-m}{1-n} \\ G_c & if \ \frac{\Delta a}{l_c} \ge \frac{3}{2}\frac{1-m}{1-n} \end{cases}$$

Inter-laminar parameters

Toray 3252S-10 (T700/2592)

*MAT_COHESIVE_MIXED_MODE (138)

Card 1

E_N	E_T	G_{IC}	G_{IIC}

Double-Cantilever Beam test

Card 2

T	S

tensile coupon test in 90 direction

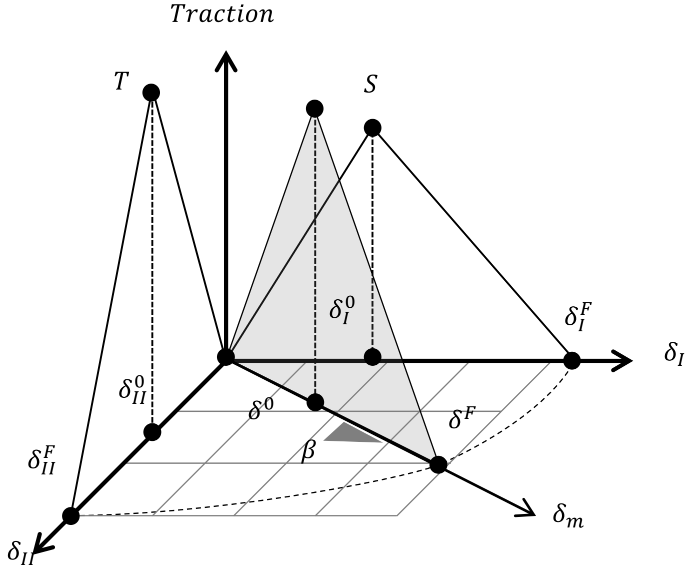

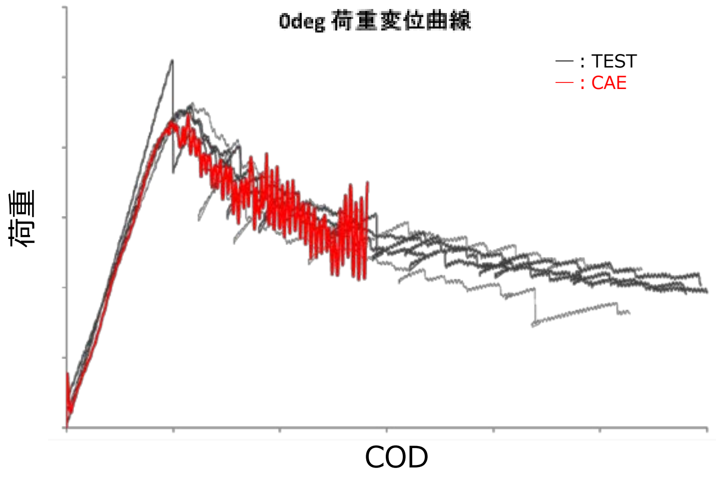

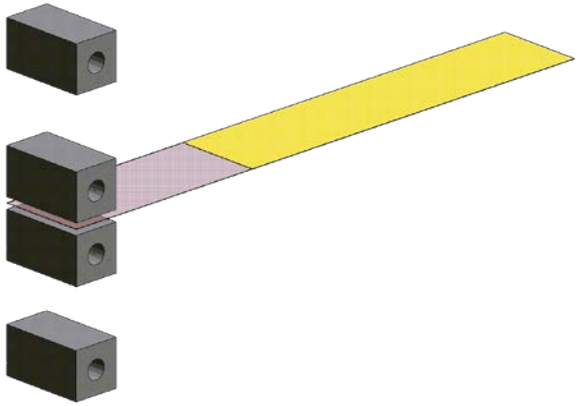

Inter-laminar parameters

Toray 3252S-10 (T700/2592)

***MAT_COHESIVE_MIXED_MODE (138)**

Card 1

E_N	E_T	G_{IC}	G_{IIC}

Card 2

T	S

tensile coupon test in 45 direction

4-point End Notched Flexure test

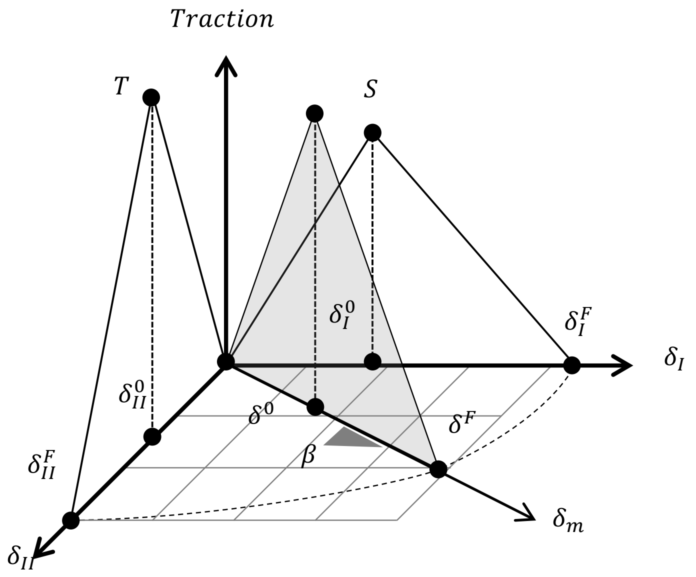

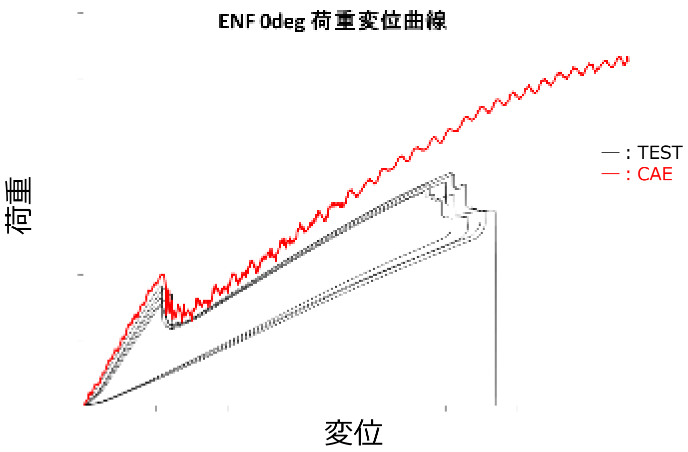

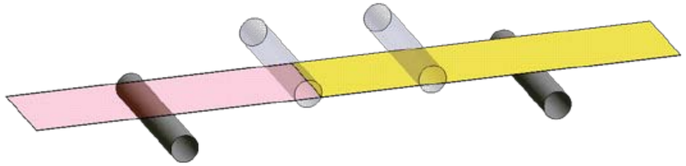

Outline

1. Background & Motivation
2. FE Modeling
3. Material Characterization
4. **1st Experimental Validation**
5. Review and Improvement of FE Modeling
6. 2nd Experimental Validation
7. Summary & Future Work

Test setup of 4-point bending of UD laminate beam

Four-point bending test was performed quasi-static (20 mm / min) using a universal testing machine.

- Location: Mazda Motor Corporation
- Equipment: Universal testing machine UH200XR (Shimadzu)

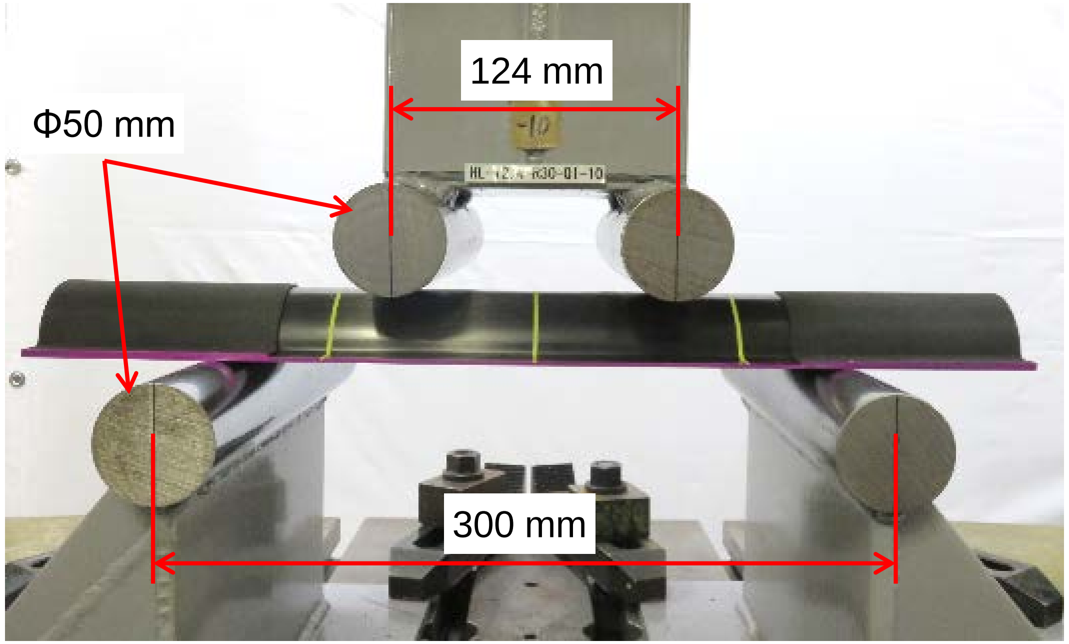

Dimension of UD laminate beam

Specimens with two types of laminated configuration were tested: quasi-isotropic and 0° main laminates.

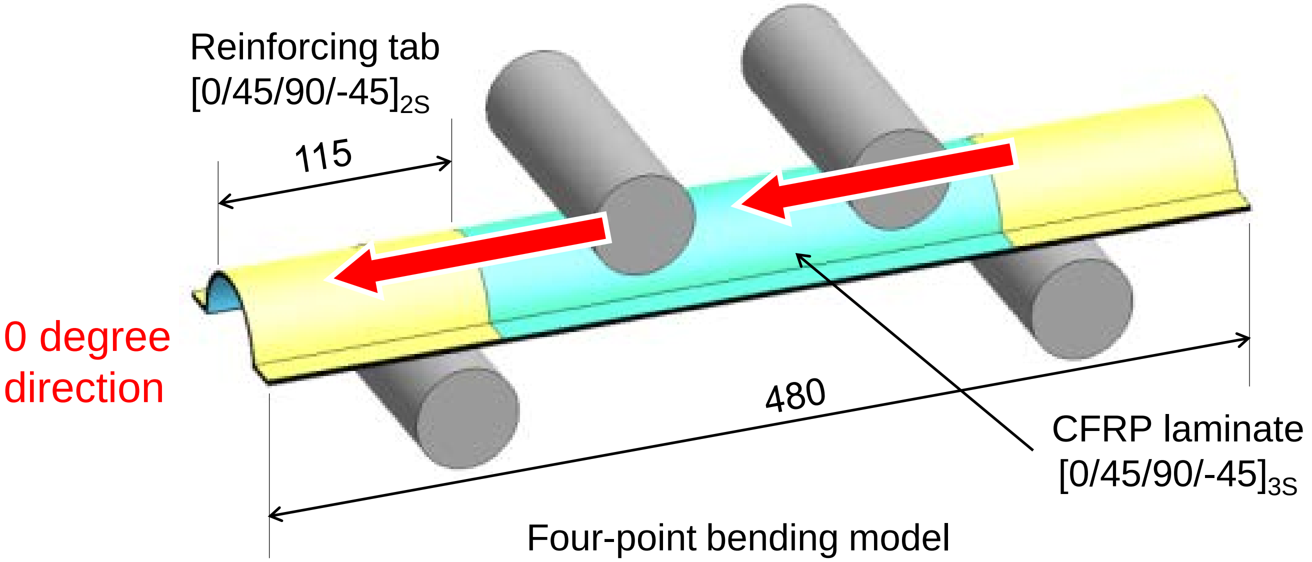

Four-point bending model

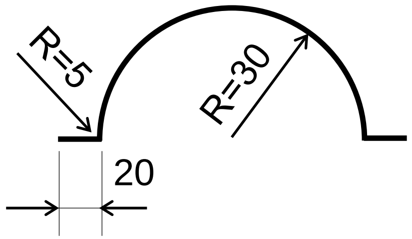

Cross section

Laminated configuration

① quasi-isotropic laminate [0/45/90/-45]$_{3S}$

② 0° main laminates [0/90/90/(0)$_9$]$_S$

Experimental results

[0/45/90/-45]$_{3S}$: Quasi-Isotropic laminate

From 10mm displacement, we obtained the crack propagated from under the impactor in the circumferential direction.

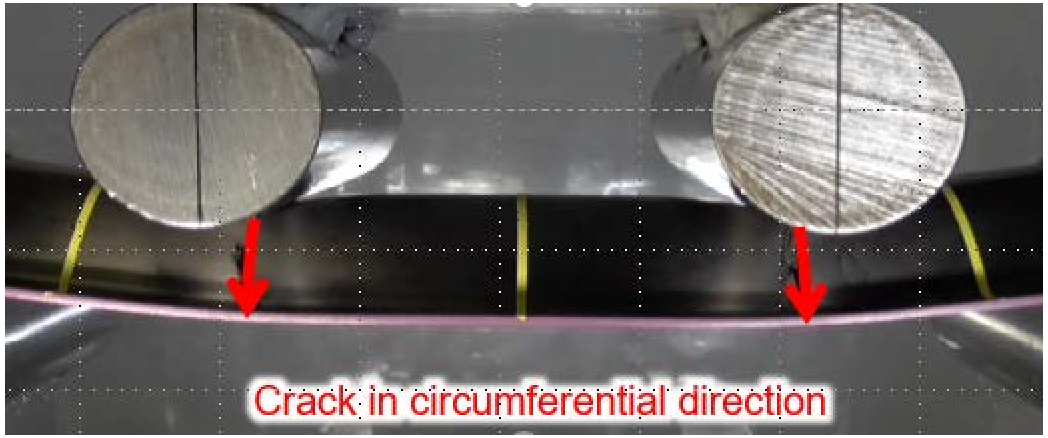

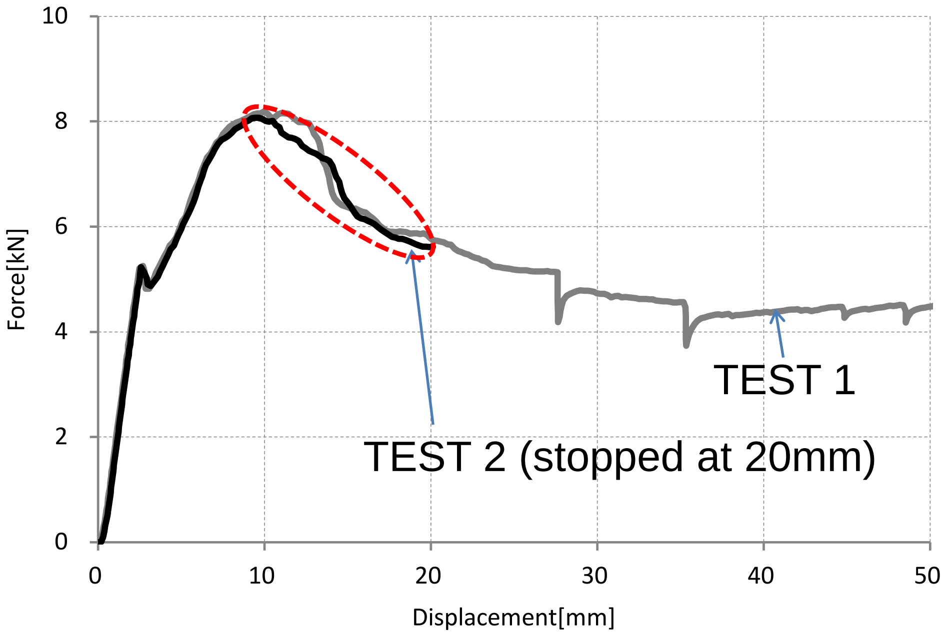

The fracture occurs on the surface at the edge of the depression, and it propagates in the circumferential direction

Model Overview

of layer : 24

- Mesh size : 1mm
- Total # of elem. : 4,069,120
  - shell：2,067,200
  - cohesive：2,001,920
- Time step : 3.0E-8 s
- LS-Dyna Version: mpp s dev
  - Shell ELFORM=16
  - CZM ELFORM=20
- Velocity of impactor
  - Test (quasi-static) : 20mm/min
  - Simulation : 2.2m/s

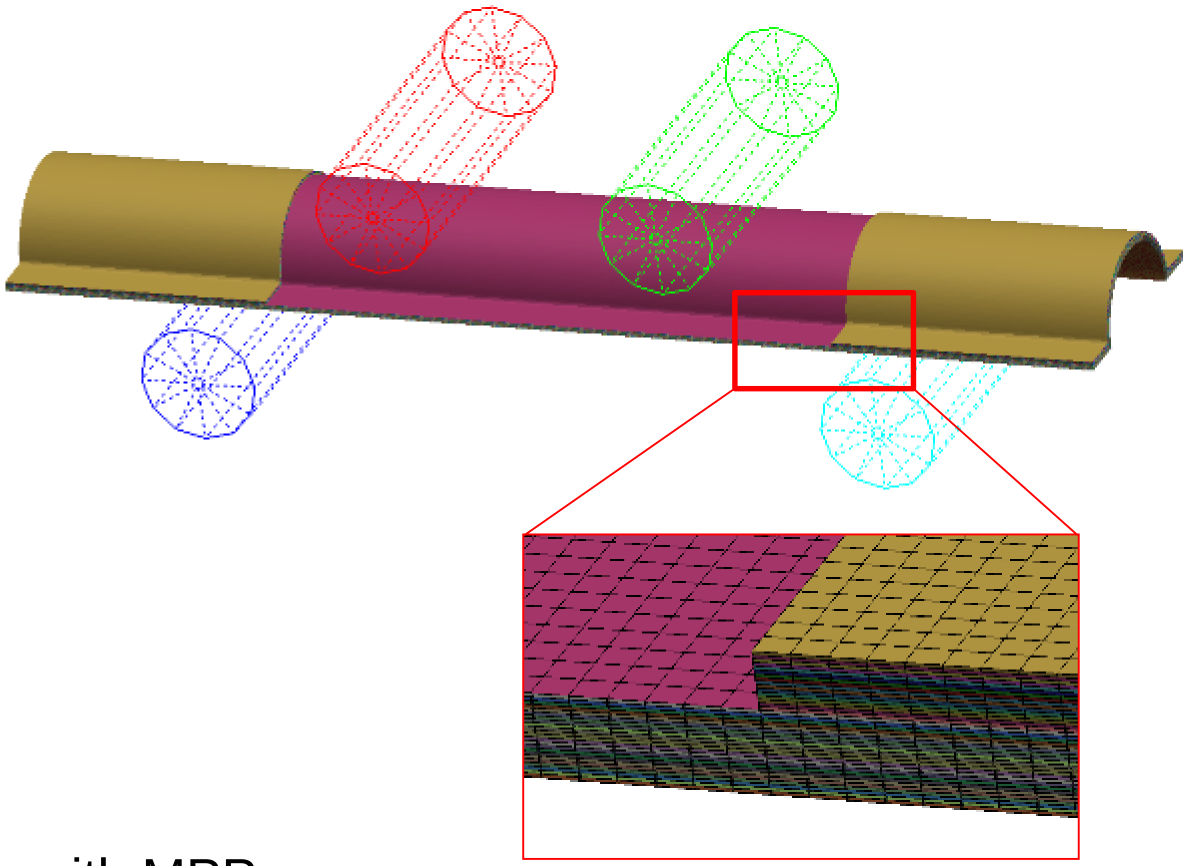

- Computational Cost : 26 hours by 128 cores with MPP

Comparison between Exp. and Sim.

QI : $[0/45/90/-45]_{3S}$ (# of layer : 24)

Force – Disp.

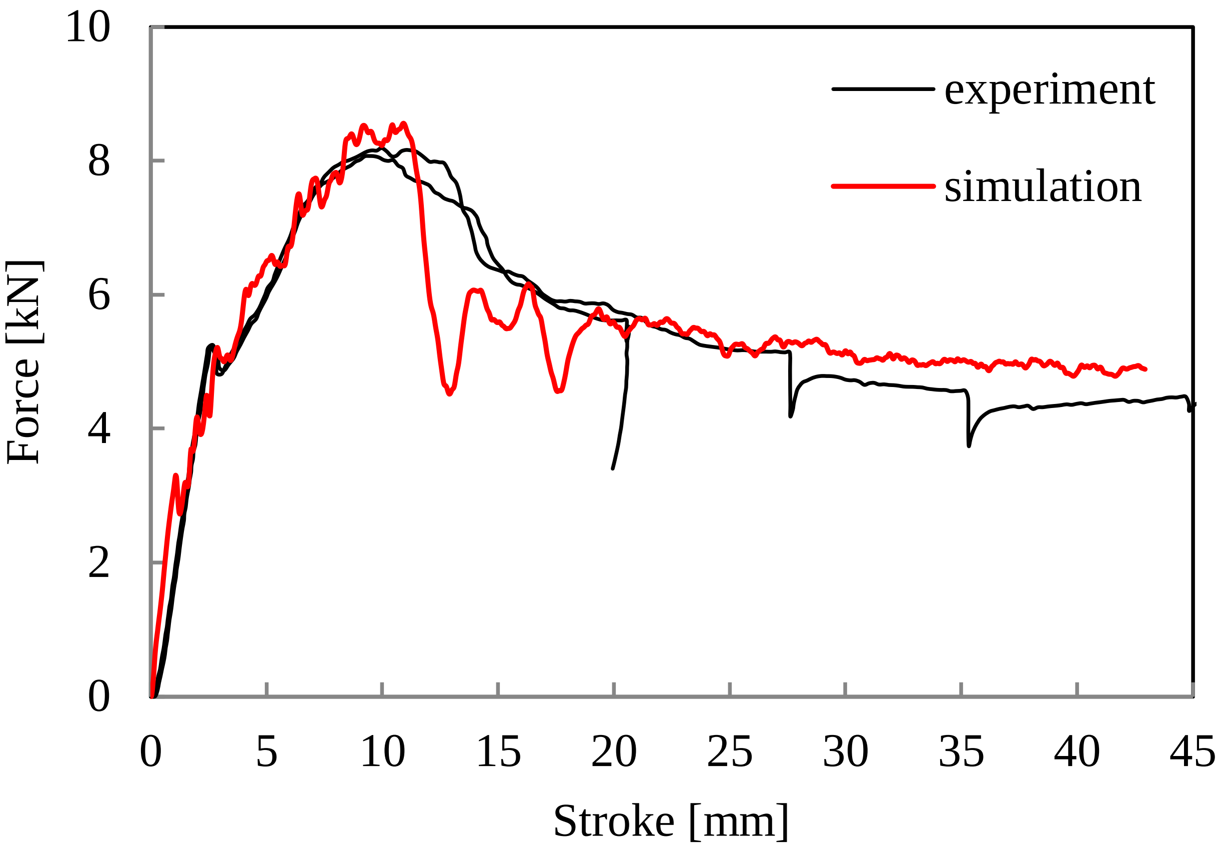

We can see good agreement with the load response obtained in the experiment, where the load gradually decreases after the maximum load is shown around 8kN.

Comparison of Crack and Damage Progress

QI : $[0/45/90/-45]_{3S}$ (# of layer : 24)

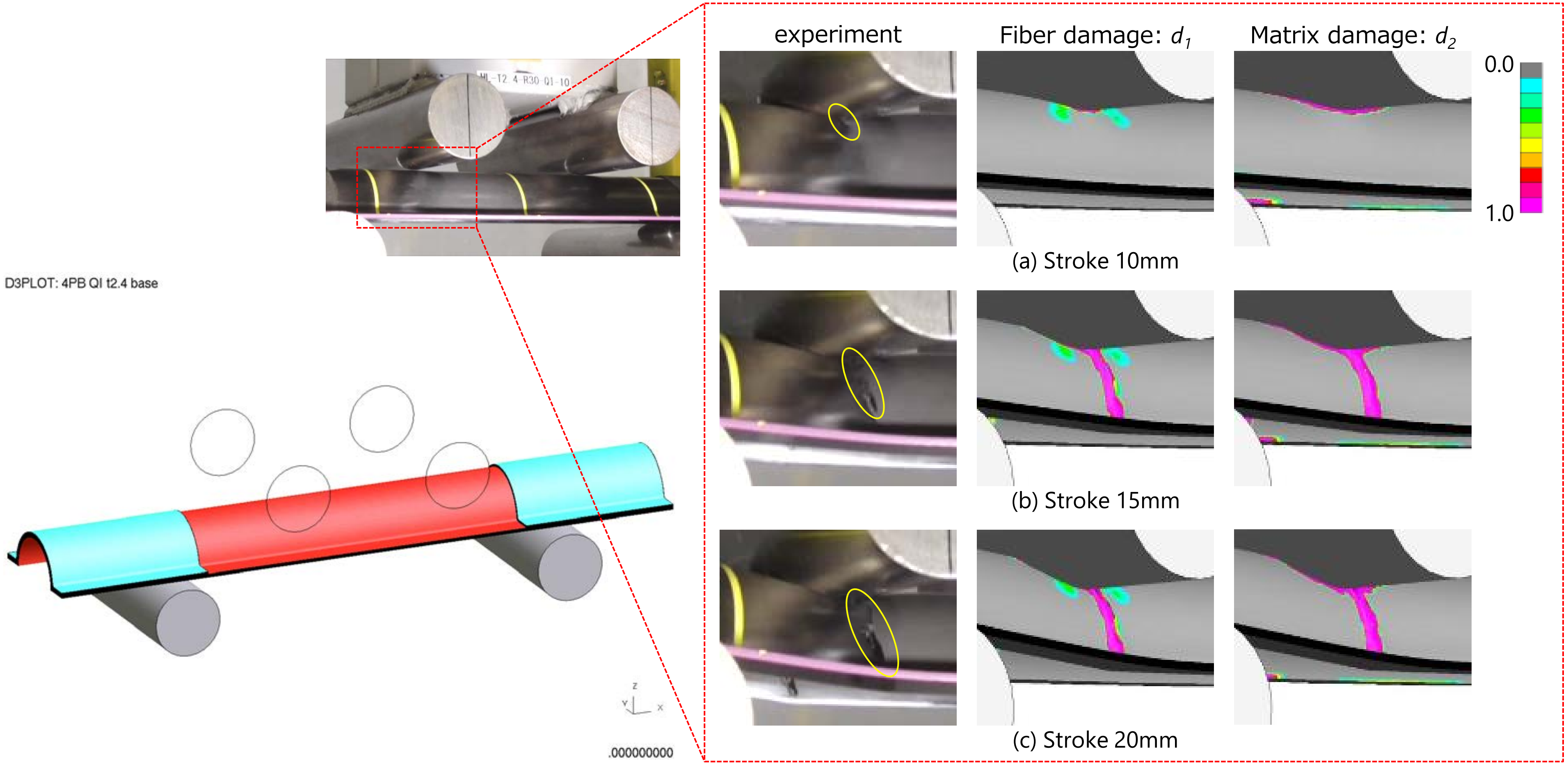

We can confirm that the simulated initiation point and the crack propagation path are in good agreement with the bending experiment.

Experimental results

$[0/90/90/(0)_9]_S$: 0 degree main laminate

Cracks propagated in the longitudinal direction and a significant decrease in load were observed.

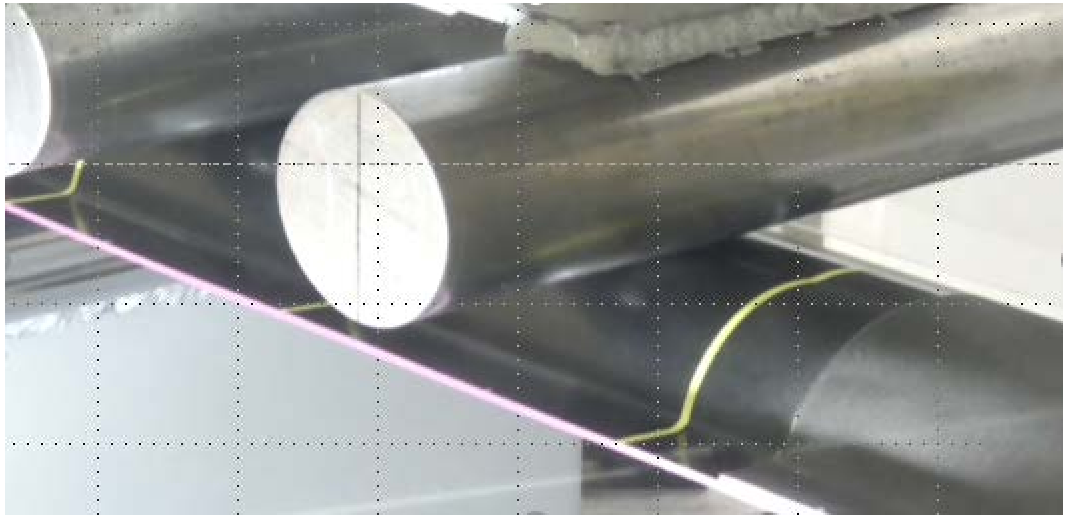

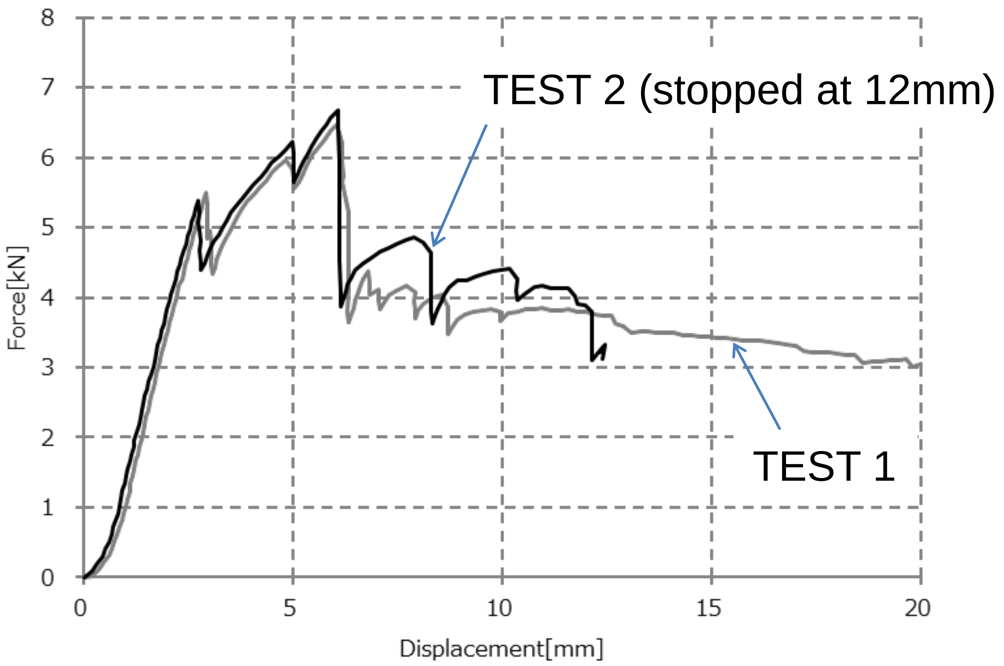

Experimental results

Comparison between quasi-Isotropic and mainly 0 degree laminates

Different failure modes were obtained depending on the laminate configuration.

Quasi-isotropic: fracture in circumferential direction

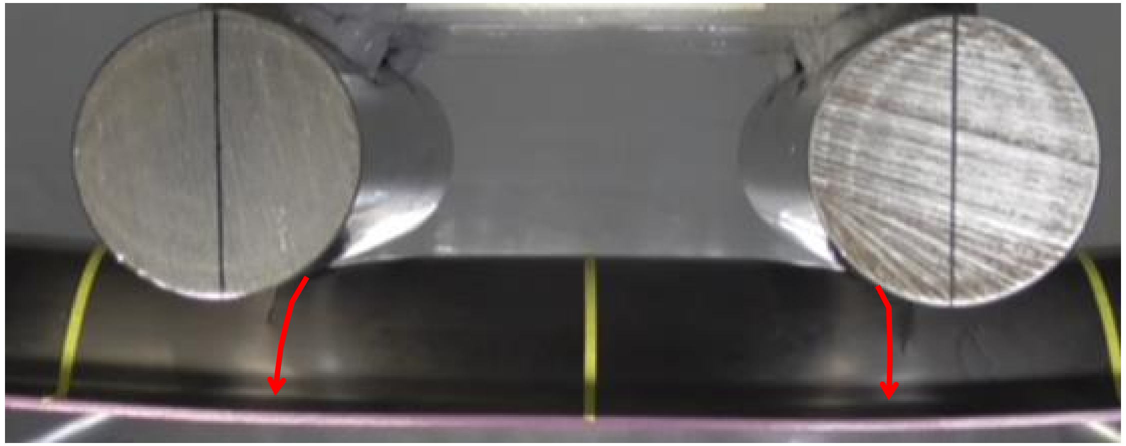

0 ° main laminate: fracture in longitudinal direction

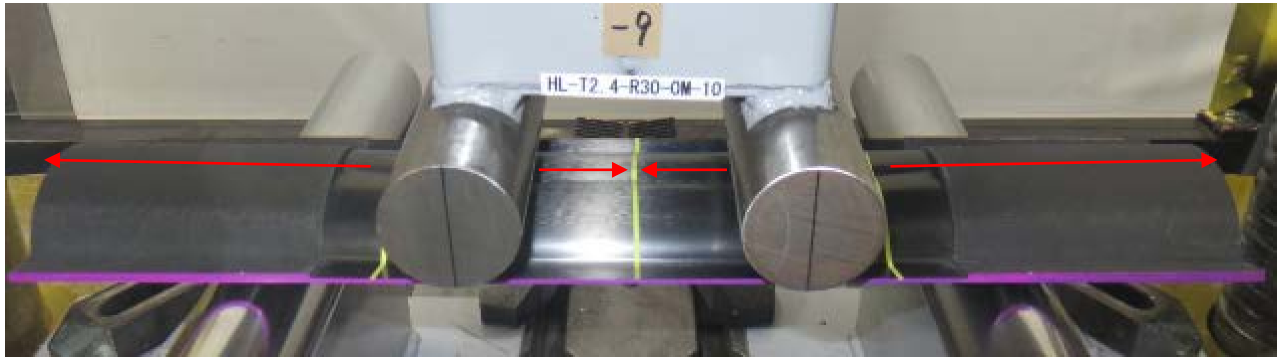

Comparison between Exp. and Sim.

0M : $[0/90/90/(0)_9]_S$(# of layer : 24)

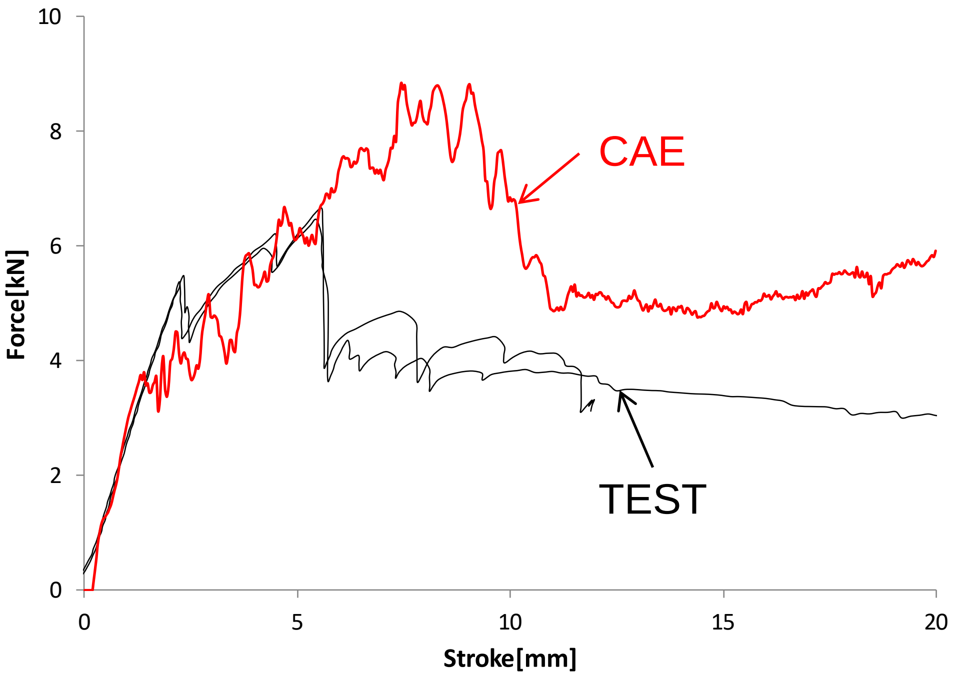

Crack in longitudinal direction is observed in experiment

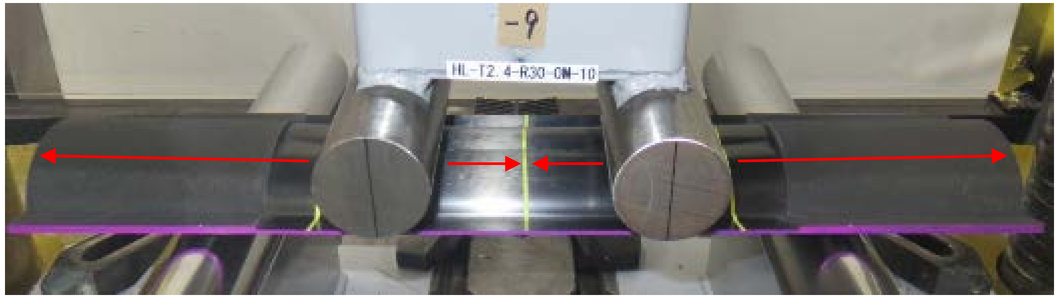

Depression under impactor and fracture progresses in the circumferential direction

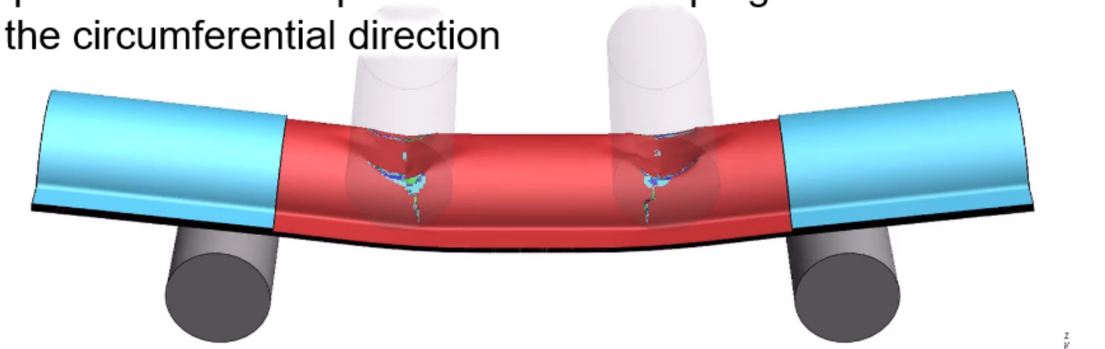

Simulated failure mode and load response cannot capture the experimental response.
The rapid load drop in the experiment cannot be reproduced in the simulation.

Outline

1. Background & Motivation
2. FE Modeling
3. Material Characterization
4. 1st Experimental Validation
5. **Review and Improvement of FE Modeling**
6. 2nd Experimental Validation
7. Summary & Future Work

Review point 1: Intra-laminar modeling

Specimen is photographed with X-ray CT to analyze the inside fractures.

- SHIMADZU inspeXio SMX-225CT FPD HR

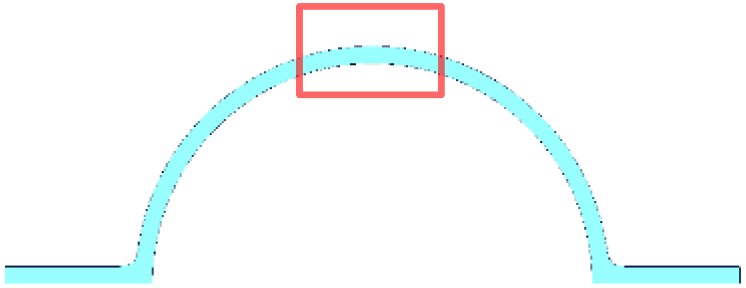

QI : $[0/45/90/-45]_{3S}$

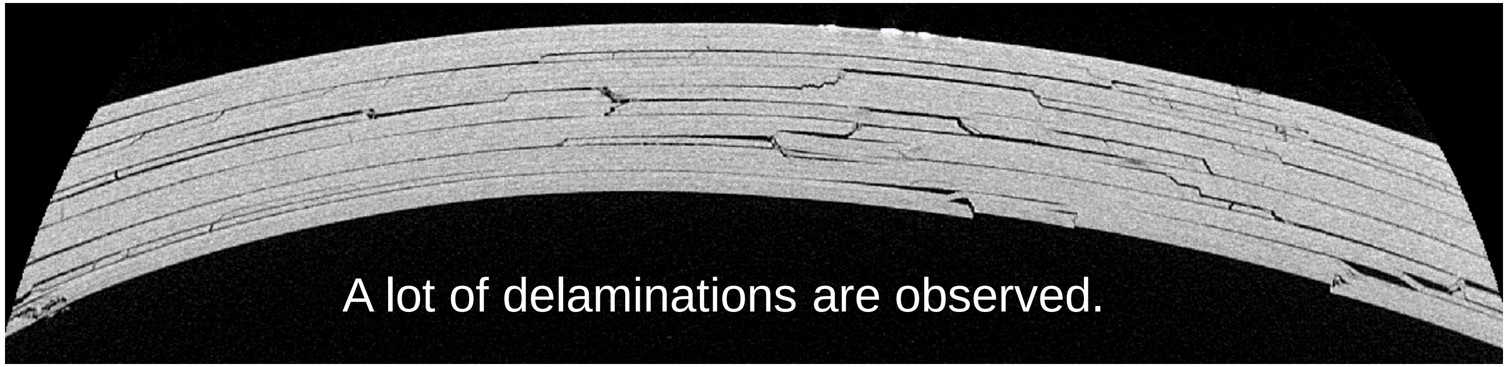

0M : $[0/90/90/(0)_9]_S$

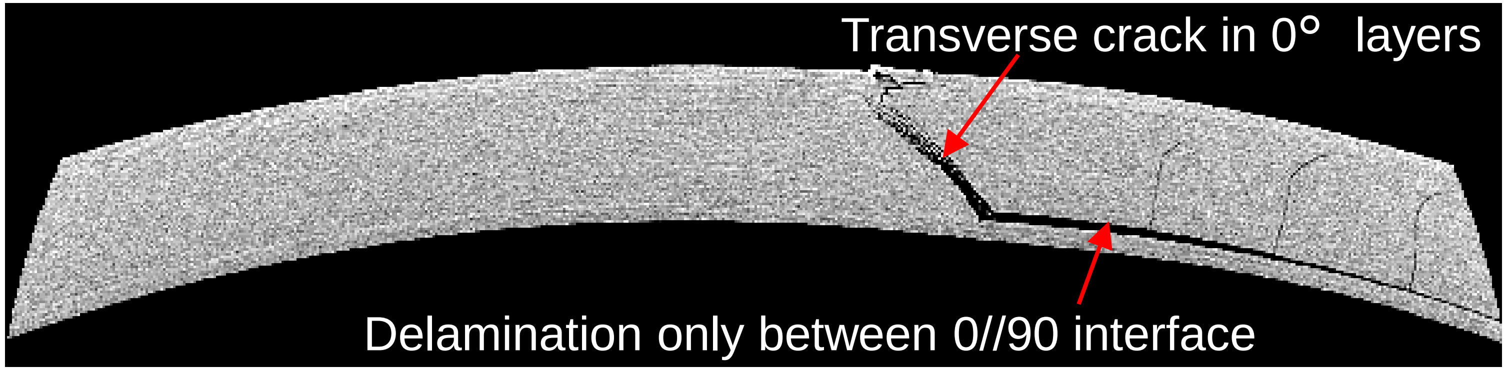

Review point 1: Intra-laminar modeling

To confirm the cause of transversal cracks observed in 0M, a detailed model with fine solid elements is conducted to confirm stress/strain distributions

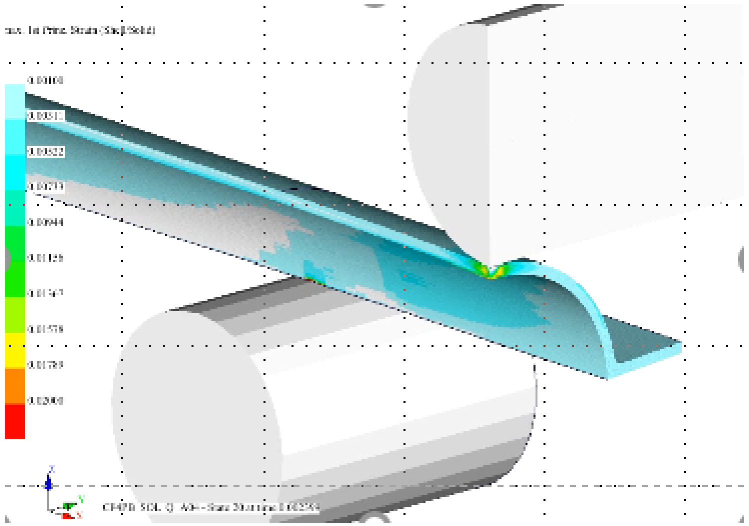

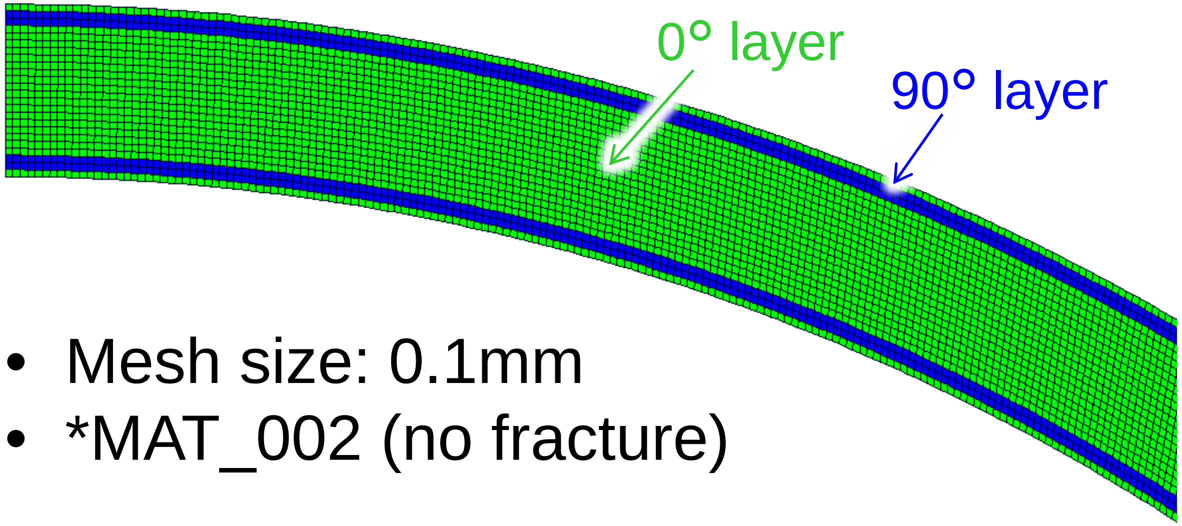

- Mesh size: 0.1mm
- *MAT_002 (no fracture)

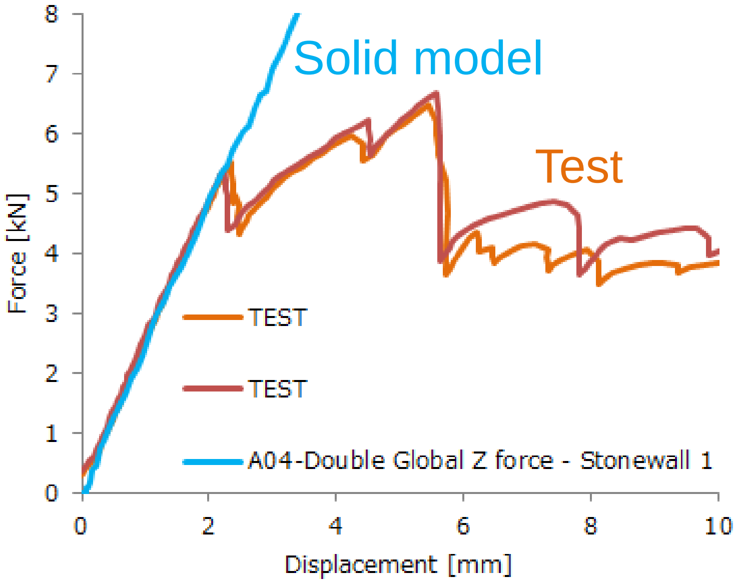

Review point 1: Intra-laminar modeling

According to the results, the cause of the initial fracture point in 0M is out-of-plane transverse shear in the lower 0 ° layer.

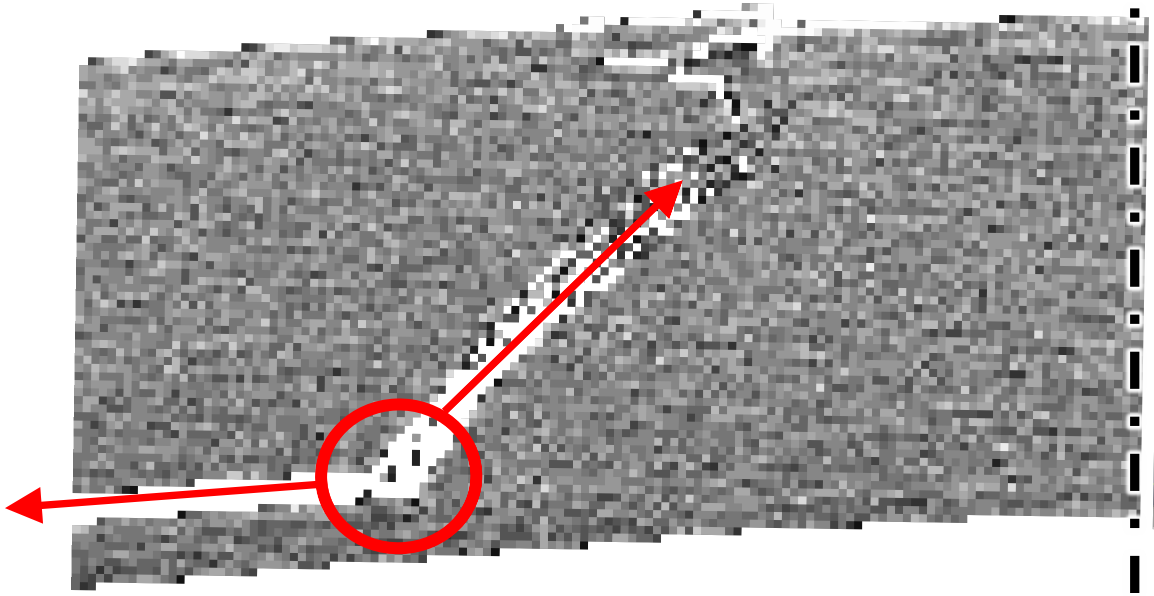

Experiment
X-CT

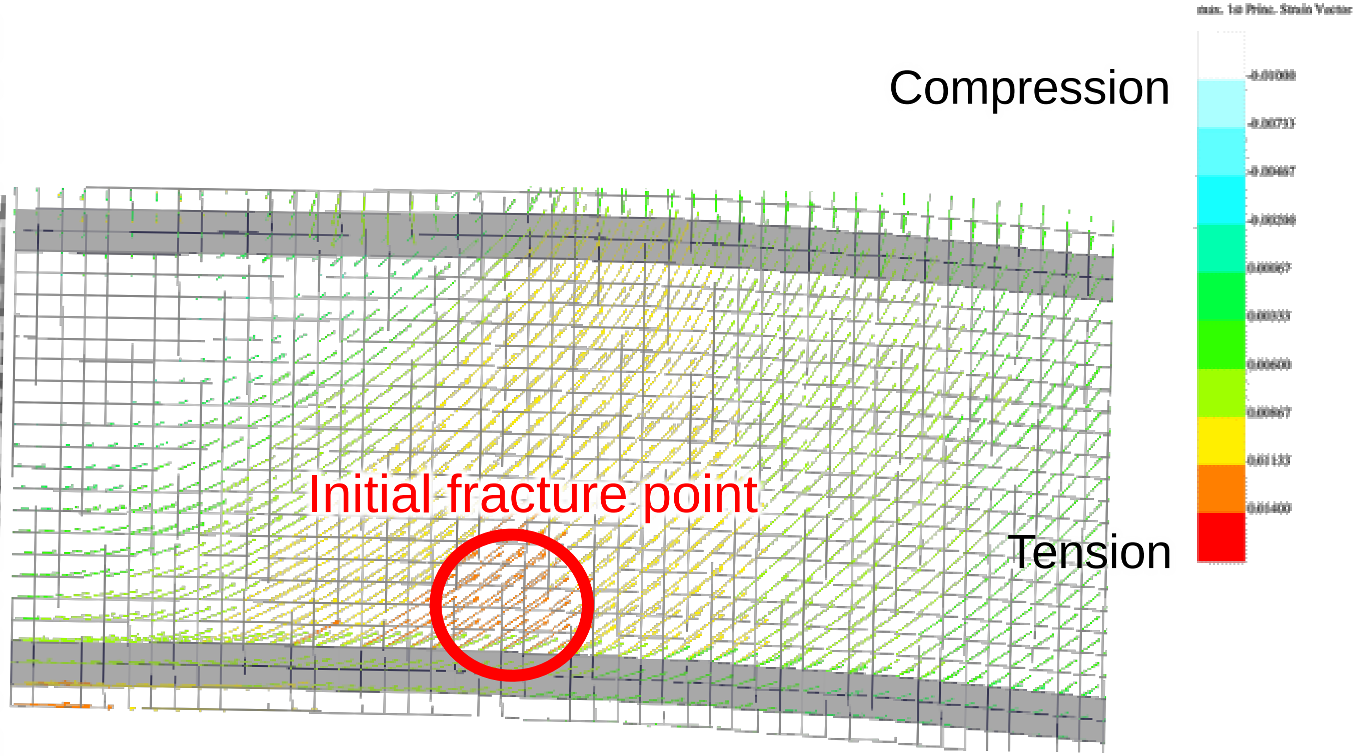

Detailed solid model
principle strain vectors

Improvement point 2: Intra-laminar modeling

To represent the transverse shear crack, transverse damage was added to *MAT_262.

Card 1. This card is required.

MID	RO	EA	EB	EC	PRBA	PRCA	PRCB

Card 2. This card is required.

GAB	GBC	GCA	AOPT	DAF	DKF	DMF	EFS

Card 3. This card is required.

XP	YP	ZP	A1	A2	A3	DSF	

Card 4. This card is required.

V1	V2	V3	D1	D2	D3	MANGLE	MSG

Card 5. This card is required.

GXC	GXT	GYC	GYT	GSL	GXCO	GXTO	

Card 6. This card is required.

XC	XT	YC	YT	SL	XCO	XTO	

Card 7. This card is required.

FIO	SIGY	ETAN	BETA	PFL	PUC	[illegible]	DT

New optional card

Card 8. This card is optional.

EPSF23	EPSR23	TSMD23	EPSF31	EPSR31	TSMD31		

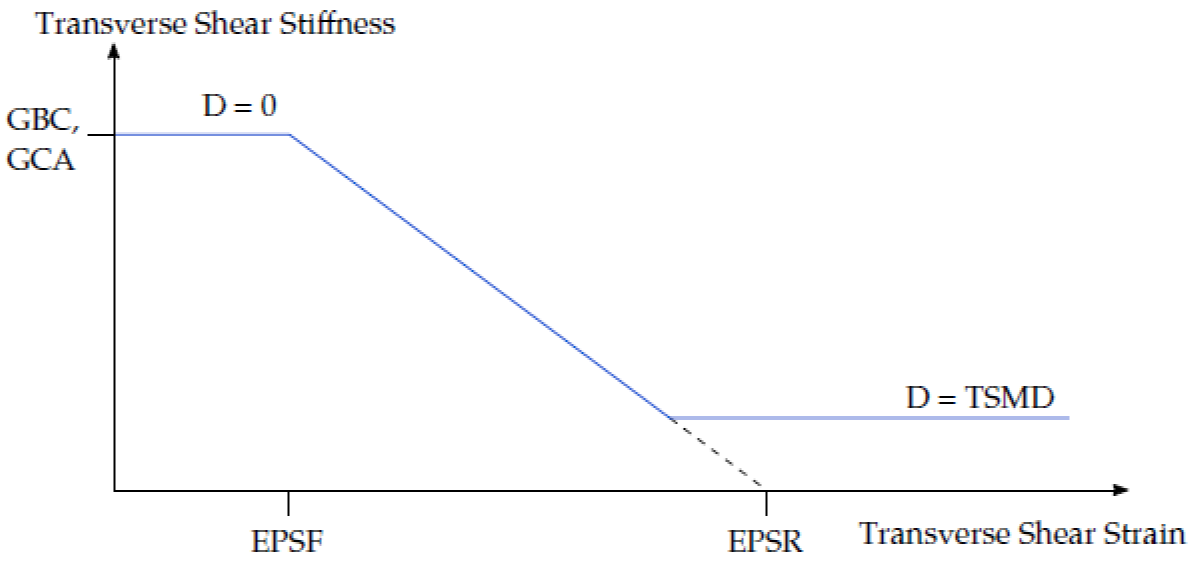

Figure M262-1. Linear Damage for Transverse Shear Behavior

Dr. Stefan Hartmann with DYNAmore kindly implemented transverse shear damage for 23-plane and 31-plane, according to our request.

Review point 2: Inter-laminar modeling

The delamination occurs before the transverse fracture within 0° layers.

Damage of Cohesive Elem.

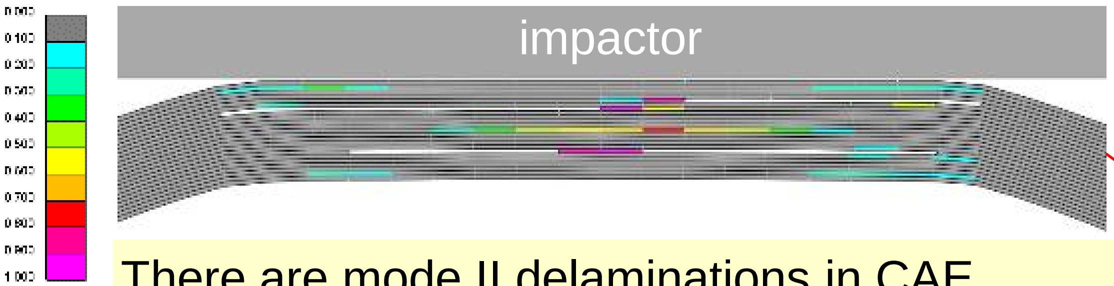

There are mode II delaminations in CAE,
but no transverse crack in thickness direction.

0M : $[0/90/90/(0)_9]_S$

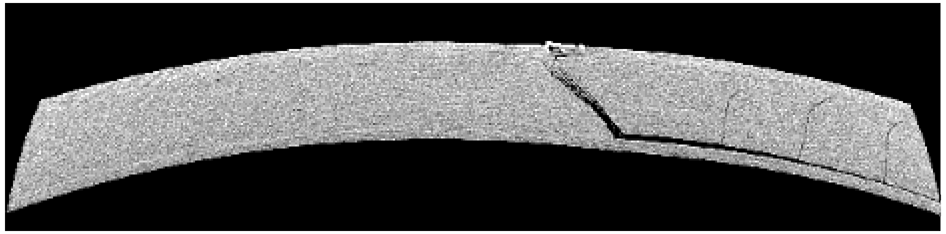

Mode II delamination is only located at 0//90 interface,
and transverse crack is observed in 0 deg. layers.

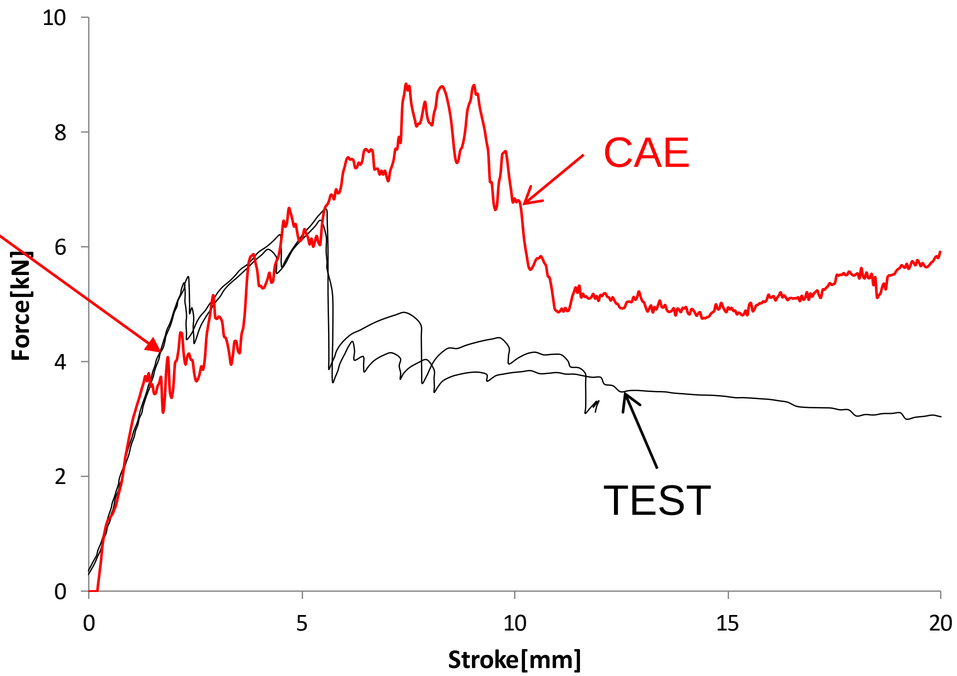

Improvement point 2: Inter-laminar modeling

Some literatures reported that the fracture toughness is larger when delamination propagates in the 90//90 direction than when propagating in the 0//0 direction.

The user defined cohesive model developed takes into account anisotropic inter-laminar fracture toughness depending on the crack propagation angle for fiber orientation.

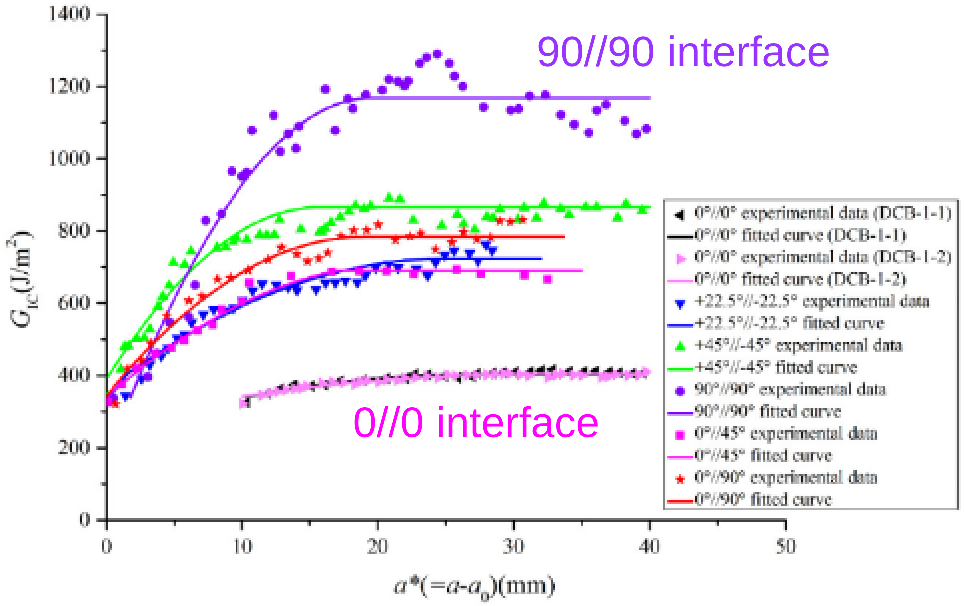

L. Zhao et al. / Composites Part B 131 (2017)

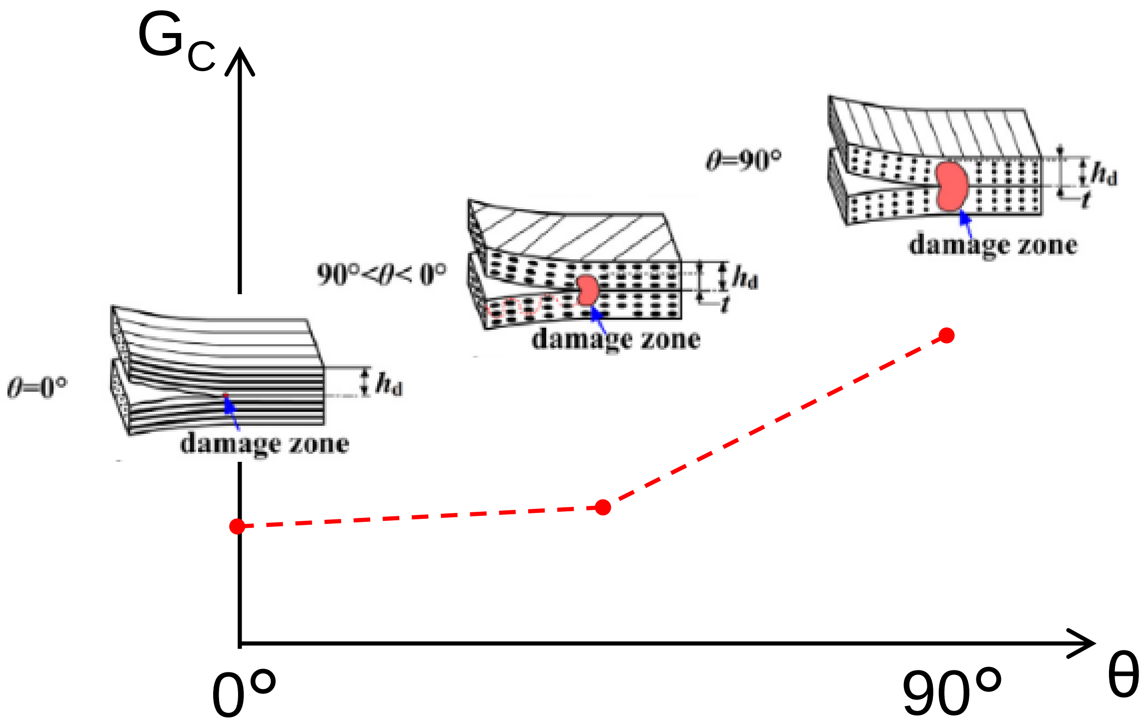

Improvement point 2: Inter-laminar modeling

Mode I opening direction is calculated from in-plane four integration points.
Mode II direction is calculated from shear deformations within each integration point.

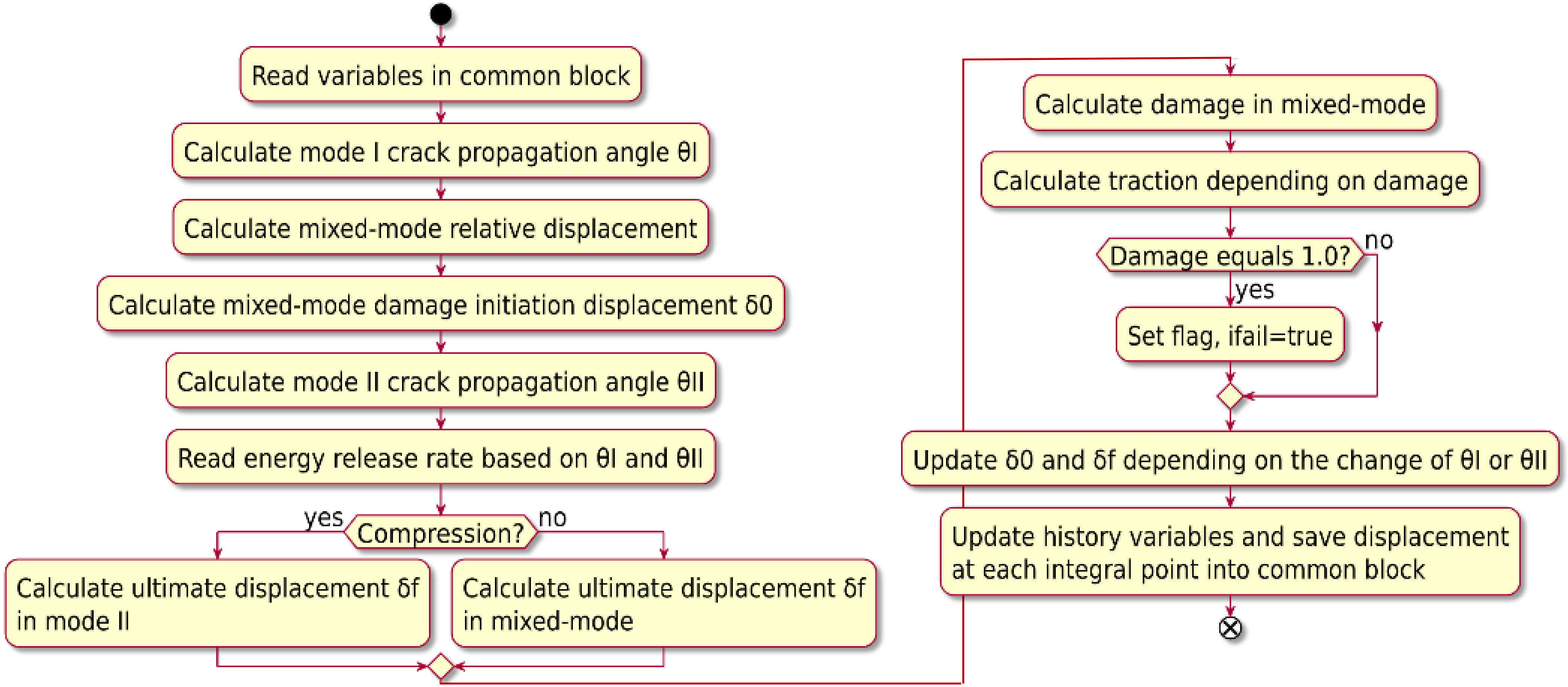

Review point 3: Laminate modeling

The upper surface is deformed
so that the cross section does not open
in the simulation.

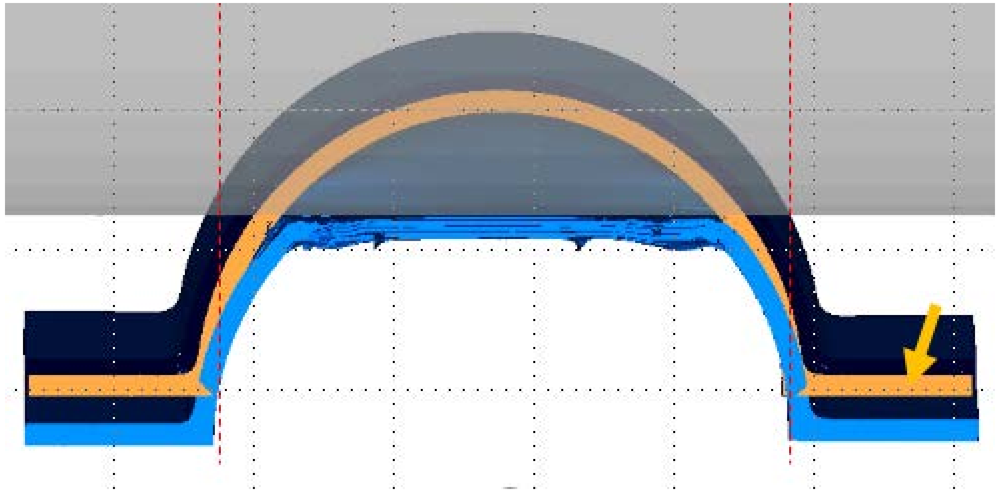

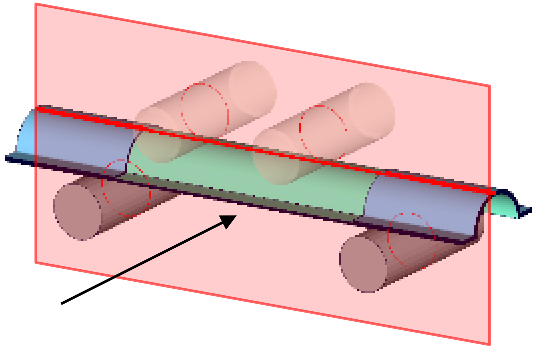

Cohesive element: rectangle

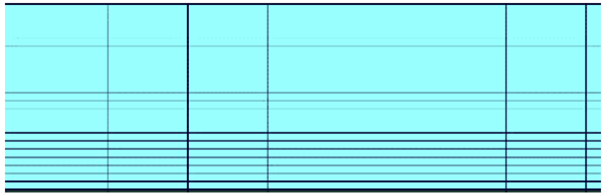

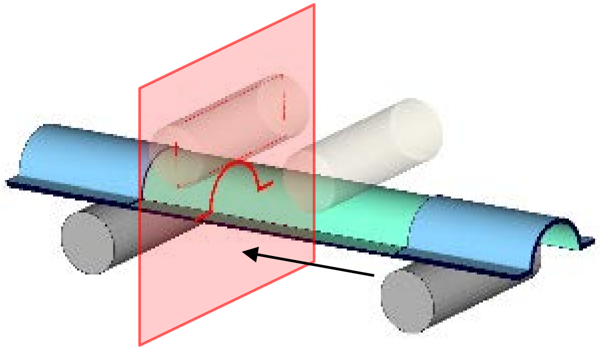

Cohesive element: inclined

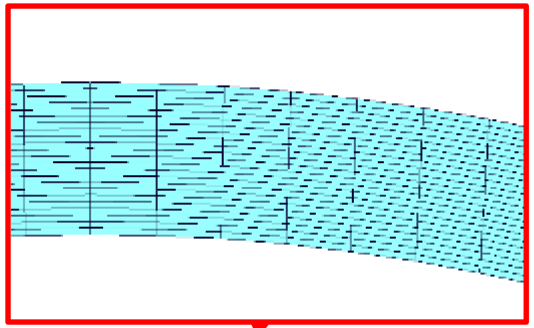

Cohesive element: inclined

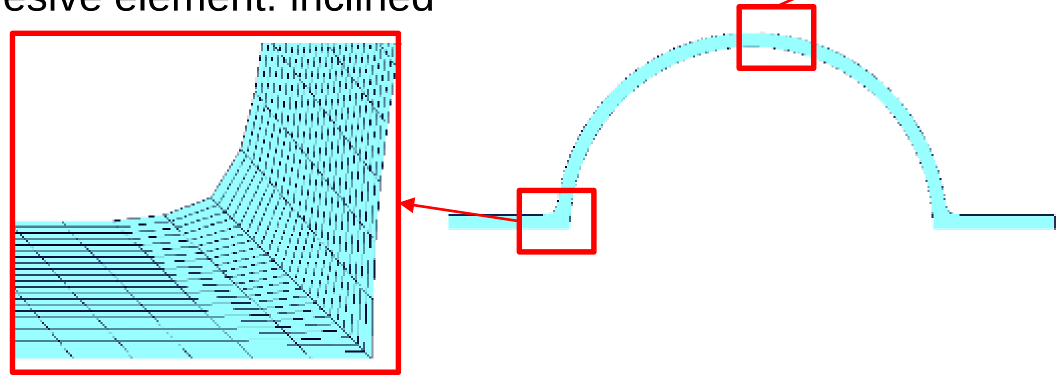

Review point 3: Laminate modeling

Numerical study

2 thin shell layers are connected by

Rectangle cohesive elements

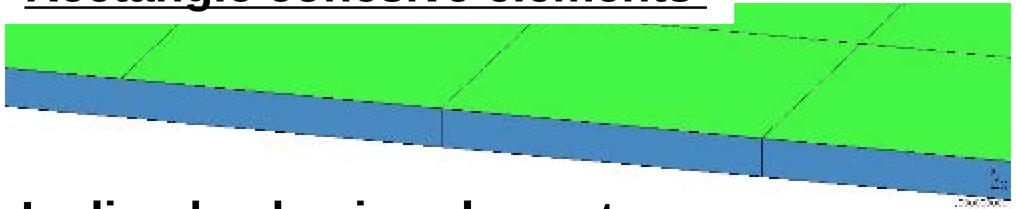

Inclined cohesive elements

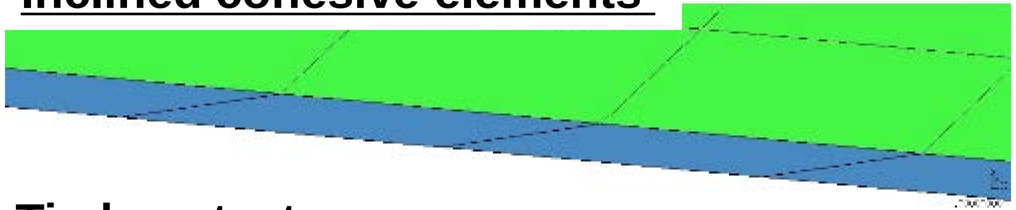

Tied contact

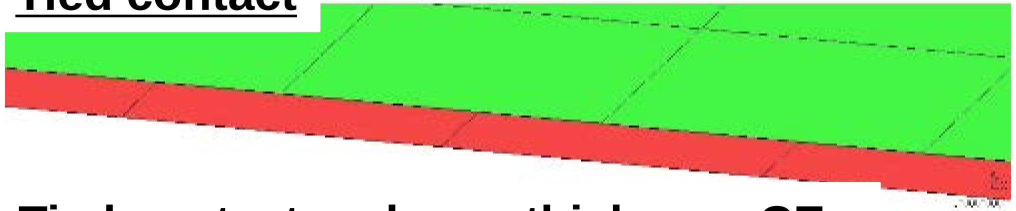

Tied contact and zero thickness CEs

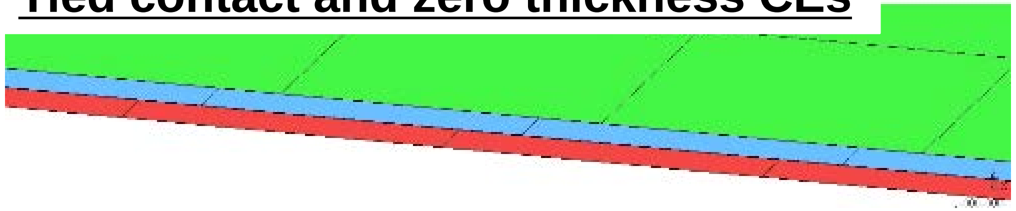

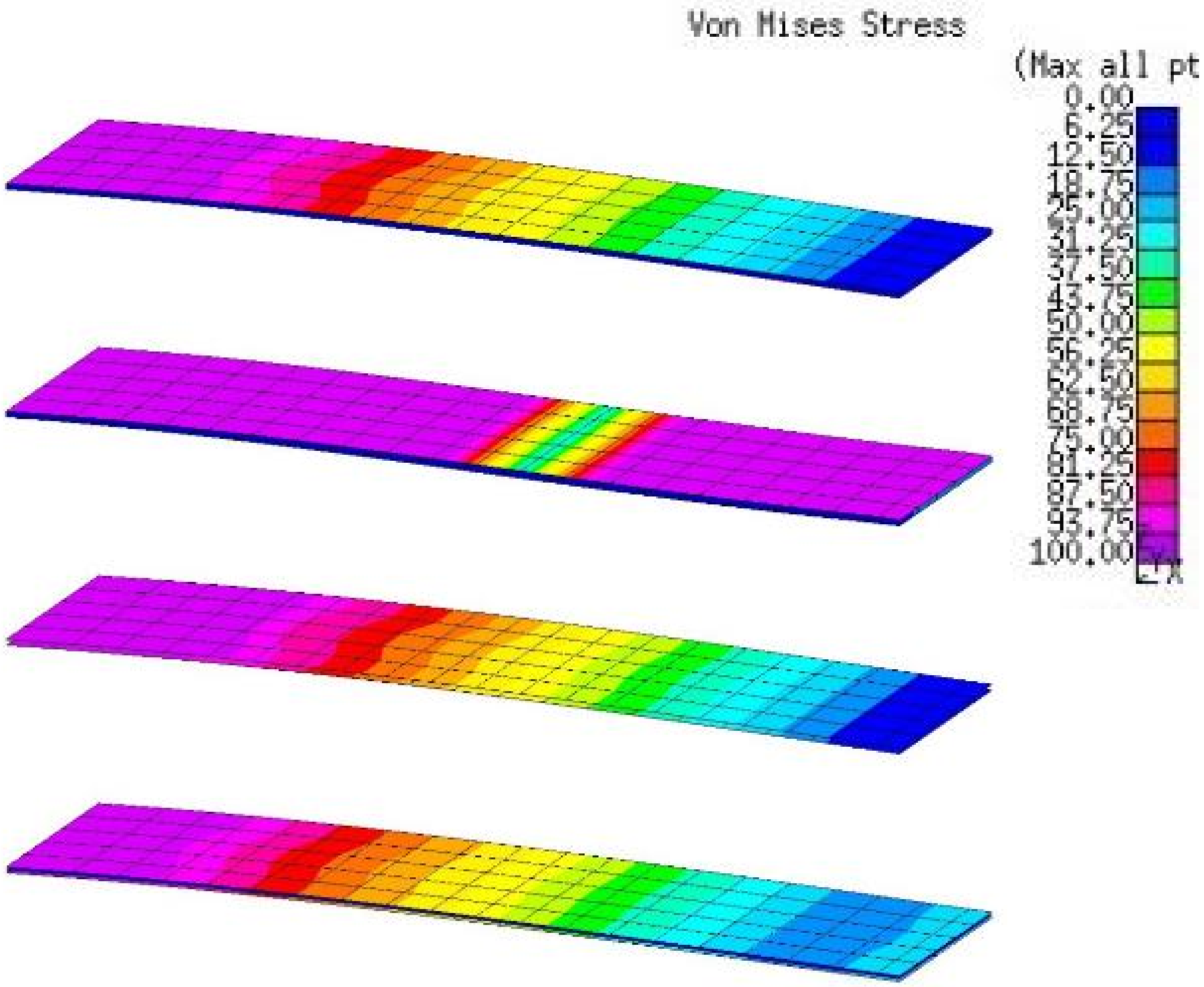

Review point 3: Laminate modeling

Numerical study

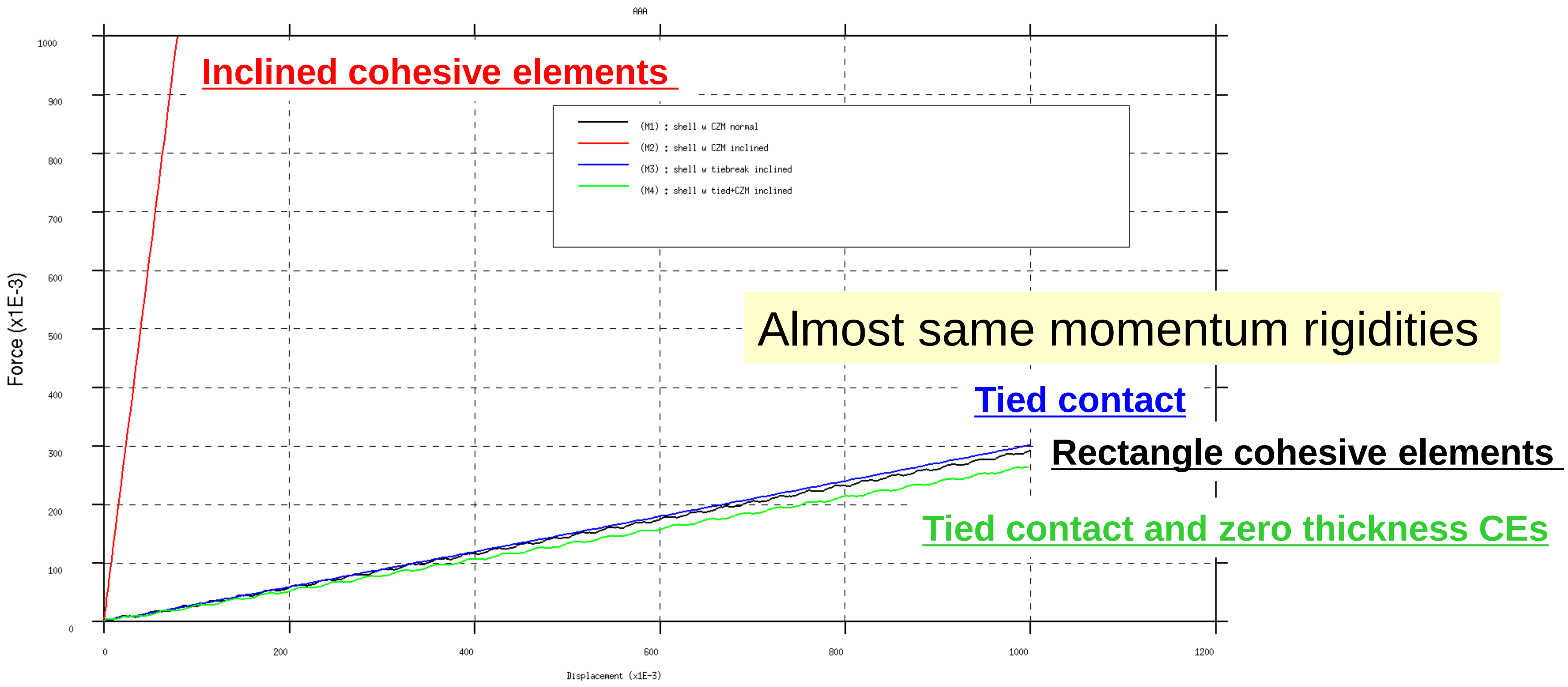

Improvement 3: Laminate modeling

Cohesive elements in the cross section of the half cylinder (left below) are inclined, not rectangular, so that the bending rigidity might increase in this section.

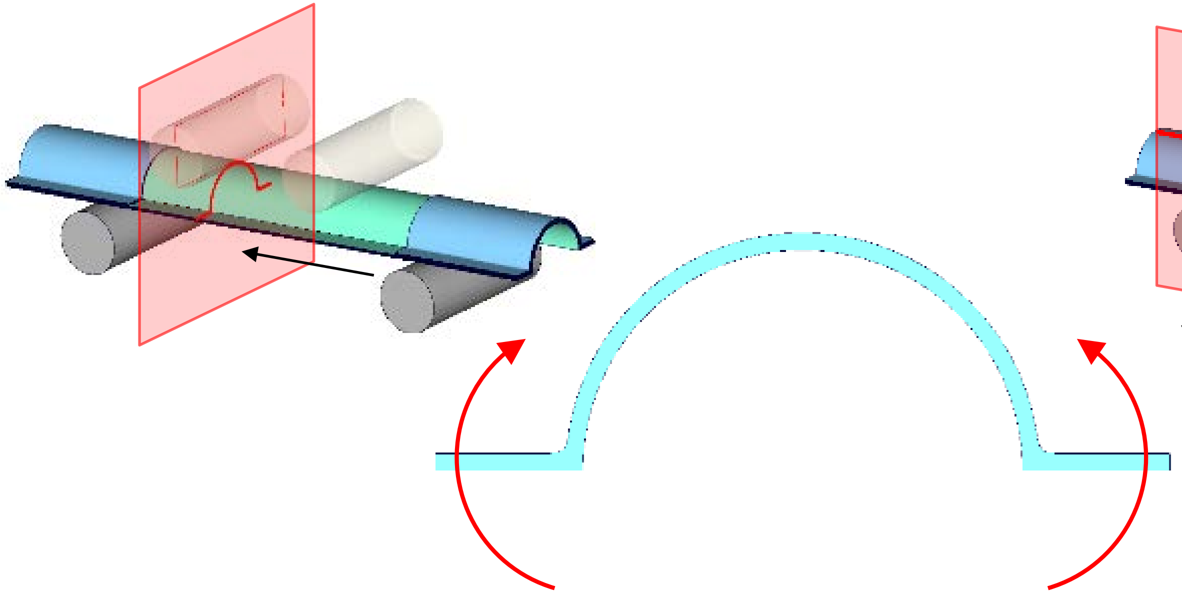

Bending rigidity in this cross section is likely to be increased. (dominant mode in 0M)

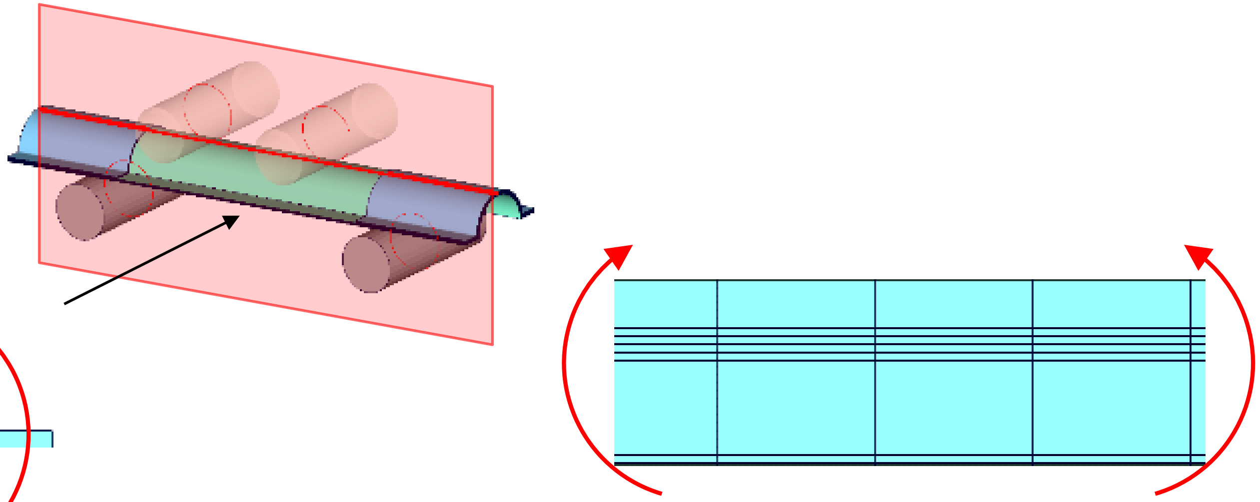

Bending rigidity in the longitudinal direction is accurately modeled with rectangle cohesive elements,
resulting in a failure mode like QI,
which is dominant in longitudinal bending

Since the numerical instability could not be overcome in the component model with tied contact and zero thickness CEs, tentatively thick shells and zero thickness shells will be used in 2nd validation model.

Outline

Model Overview

of layer : 24

- Mesh size : 1mm
- Total # of elem. : 4,069,120
  - Thick-shell：2,067,200
  - cohesive：2,001,920
- Time step : 5.0E-9 s
- LS-Dyna Version: mpp s Dev (**enhanced MAT_262**, **implemented UCZM**)
  - **Thick-Shell** ELFORM=1
  - CZM ELFORM=19 (**zero-thickness**)
- Velocity of impactor
  - Test (quasi-static) : 20mm/min
  - Simulation : 2.2m/s
- Computational Cost : 82 hours by 128 cores with MPP

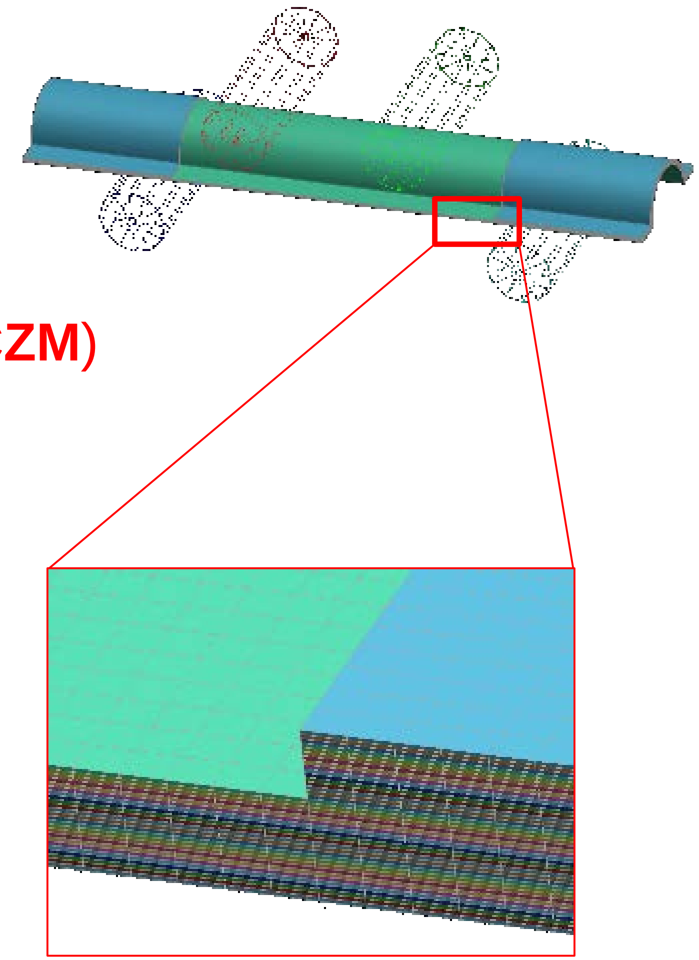

Simulated Failure Mode by Improved Model

0M : $[0/90/90/(0)_9]_S$(# of layer : 24)

Longitudinal crack growth and deformation in which the cross section opened.

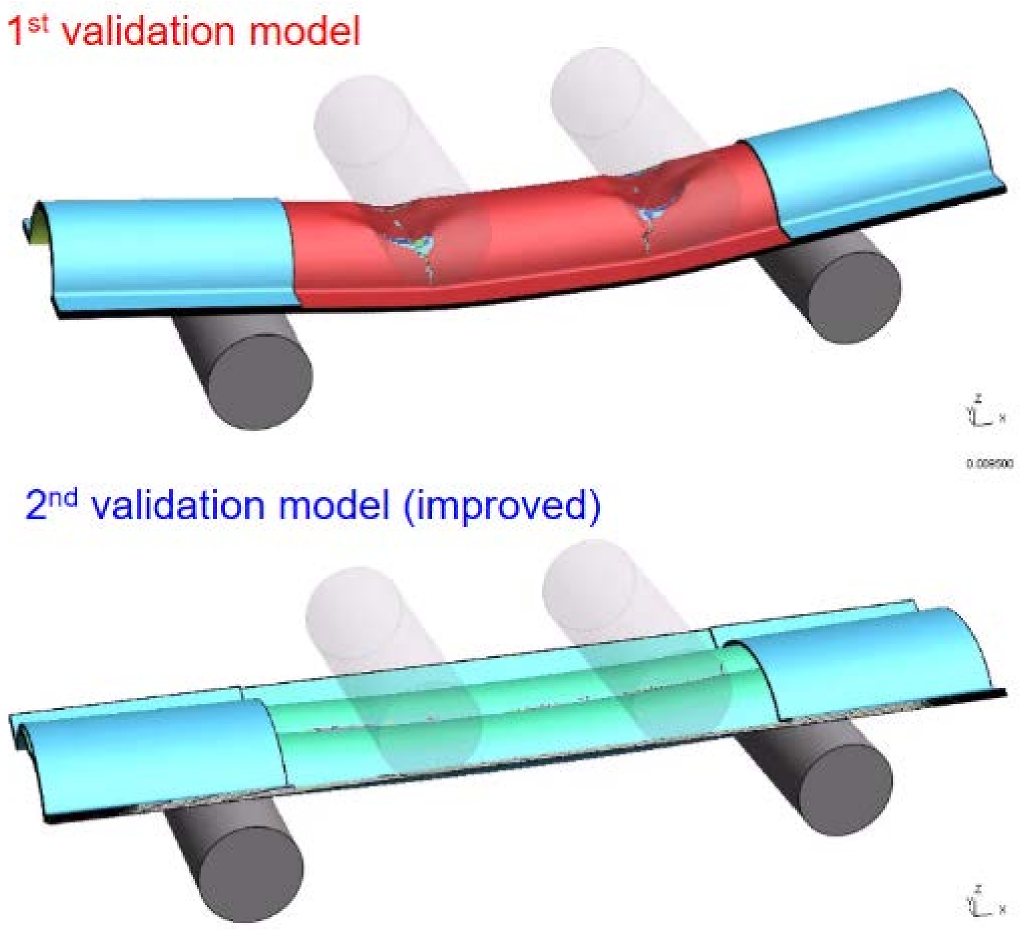

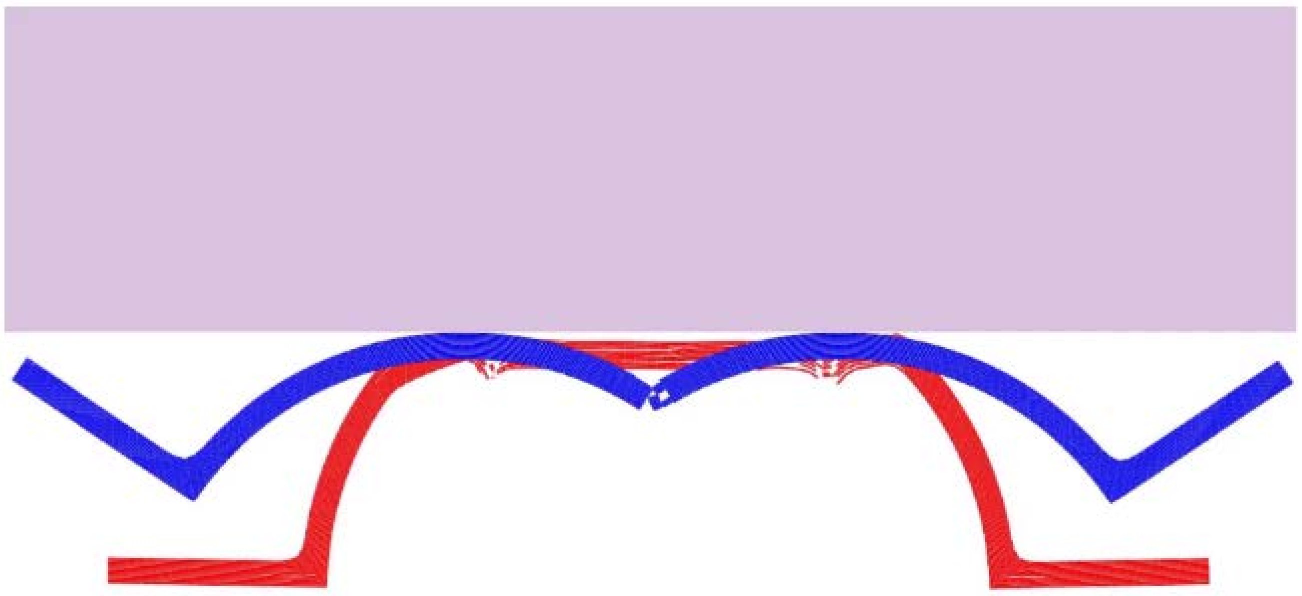

Simulated Load Response by Improved Model

0M : $[0/90/90/(0)_9]_S$(# of layer : 24)

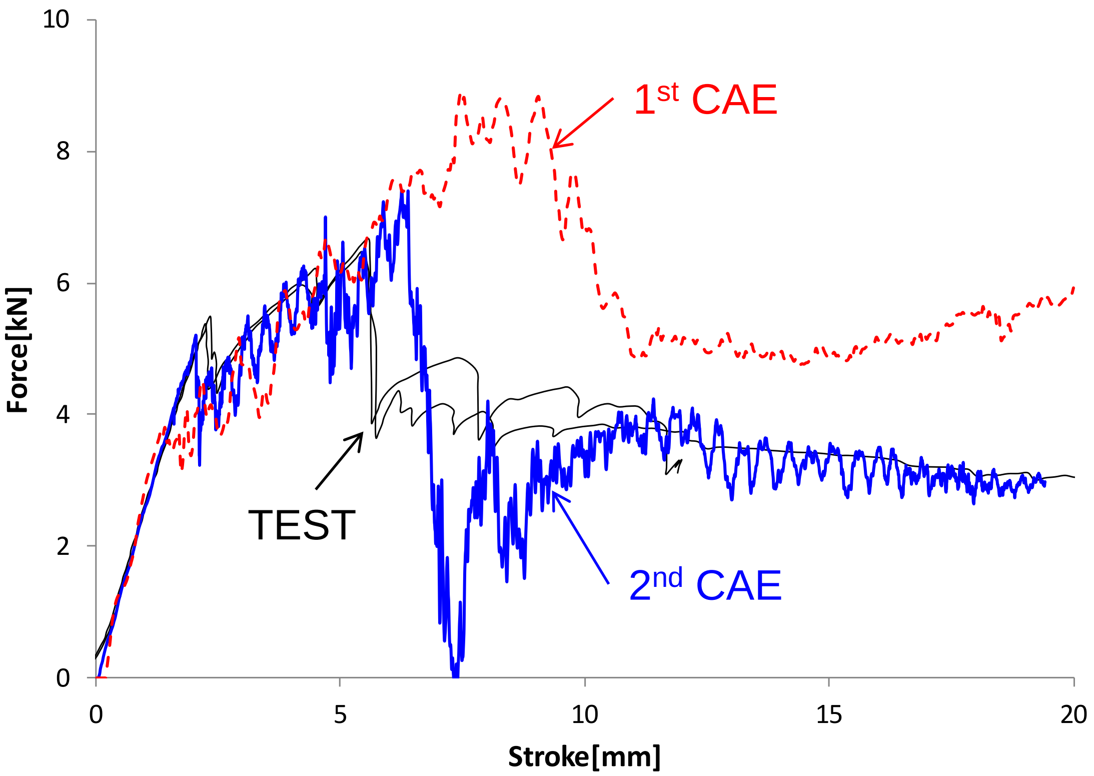

Fracture in longitudinal direction

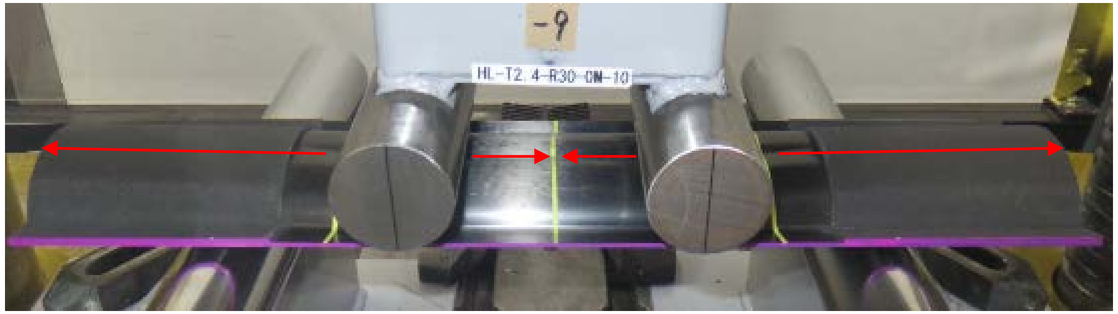

Longitudinal failure growth is represented.

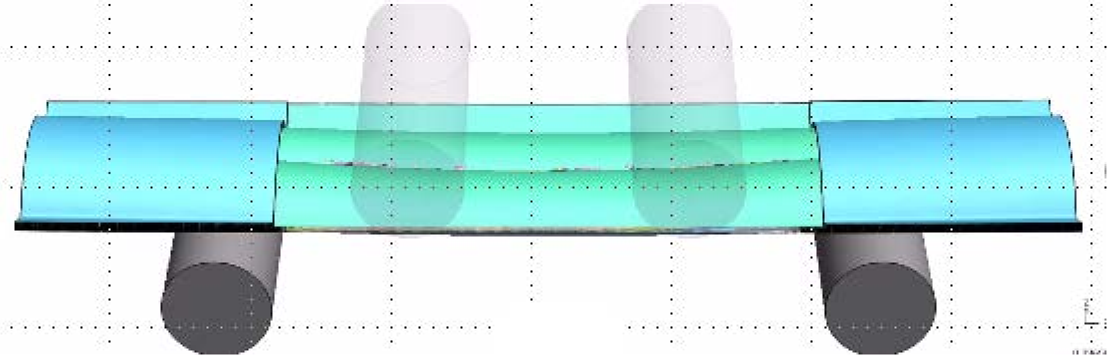

Improved CAE model in 2nd validation can capture the failure mode and load response observed in experiments.

Outline

Summary & Future Work

Summary

- Confirmed that different failure modes occur depending on the lamination configuration of UD laminate beams in four-point bending experiments.
- Analyzed the fracture mode by X-ray CT and detailed solid model.
- Represented the change in the failure mode due to the laminated configuration by improved FE model.

Future Work

- Characterization of direction-dependent inter-lamina fracture toughness.
- Improvement of numerical instability in the model with tied contact and zero-thickness cohesive elements.
- Validation for different cross sections and laminate configurations.

Thank you for your attention!